

IMAGING THE GEOMETRY OF PALEOVALLEYS IN THE SOUTHWEST REGION OF WESTERN AUSTRALIA: LINKING BASEMENT AND COVER

S Jakica, P Duuring, I González-Álvarez and JK Porter





Department of **Energy, Mines,
Industry Regulation and Safety**

REPORT 247

IMAGING THE GEOMETRY OF PALEOVALLEYS IN THE SOUTHWEST REGION OF WESTERN AUSTRALIA: LINKING BASEMENT AND COVER

S Jakica, P Duuring, I González-Álvarez¹ and JK Porter^{2,3}

1 CSIRO, ARRC, 26 Dick Perry Avenue, Kensington WA 6151

2 Future Industries Institute, University of South Australia, Mawson Lakes, SA 5095

3 MinEx CRC, ARRC, 26 Dick Perry Avenue, Kensington WA 6151

PERTH 2024



**Geological Survey of
Western Australia**

MINISTER FOR MINES AND PETROLEUM
Hon David Robert Michael MLA

DIRECTOR GENERAL, DEPARTMENT OF ENERGY, MINES, INDUSTRY REGULATION AND SAFETY
Richard Sellers

EXECUTIVE DIRECTOR, GEOLOGICAL SURVEY AND RESOURCE STRATEGY
Michele Spencer

REFERENCE

The recommended reference for this publication is:

Jakica, S, Duuring, P, González-Álvarez, I and Porter, J 2024, Imaging the geometry of paleovalleys in the southwest region of Western Australia: linking basement and cover: Geological Survey of Western Australia, Report 247, 22p.



A catalogue record for this
book is available from the
National Library of Australia

ISBN 978-1-74168-033-1

ISSN 1834-2280

Grid references in this publication refer to the Geocentric Datum of Australia 1994 (GDA94). Locations mentioned in the text are referenced using Map Grid Australia (MGA) coordinates, Zone 50. All locations are quoted to at least the nearest 100 m.

About the publication

The study presented in this Report is the result of a collaborative research project, Detection of Distal Footprints of Minerals Systems in southwest of Western Australia: Linking basement and Cover (SOWETO), with the Geological Survey of Western Australia (GSWA), CSIRO, Minerals Research Institute of Western Australia (MRIWA), Anglo America Ltd. and Ramelius Resources Ltd. The principal objective of this research is to build a contextual framework to help more efficient mineral exploration protocols in the southwest region of Western Australia. This research aims to better understand how the basement and cover variability of the area are linked, and how these links can be used to vector mineral systems at depth and in the cover.



Disclaimer

This product uses information from various sources. The Department of Energy, Mines, Industry Regulation and Safety (DEMIRS) and the State cannot guarantee the accuracy, currency or completeness of the information. Neither the department nor the State of Western Australia nor any employee or agent of the department shall be responsible or liable for any loss, damage or injury arising from the use of or reliance on any information, data or advice (including incomplete, out of date, incorrect, inaccurate or misleading information, data or advice) expressed or implied in, or coming from, this publication or incorporated into it by reference, by any person whatsoever.

Acknowledgement of Country

The Department of Energy, Mines, Industry Regulation and Safety (DEMIRS) respectfully acknowledges Aboriginal peoples as being the traditional custodians of Western Australia. We acknowledge the enduring connection Aboriginal people continue to share with the land, sea and sky through both their ancestral ties and custodianship to Country. We pay our respect to Elders both past and present, and acknowledge the value brought to our department through the collective contribution of Aboriginal and Torres Strait Islander peoples across Western Australia.

Published 2024 by the Geological Survey of Western Australia

This Report is published in digital format (PDF) and is available online at <www.demirs.wa.gov.au/GSWApublications>.



© State of Western Australia (Department of Energy, Mines, Industry Regulation and Safety) 2024

With the exception of the Western Australian Coat of Arms and other logos, and where otherwise noted, these data are provided under a Creative Commons Attribution 4.0 International Licence. (<https://creativecommons.org/licenses/by/4.0/legalcode>)

Further details of geoscience products are available from:

First Floor Counter
Department of Energy, Mines, Industry Regulation and Safety
100 Plain Street
EAST PERTH WESTERN AUSTRALIA 6004
Telephone: +61 8 9222 3459 Email: publications@demirs.wa.gov.au
www.demirs.wa.gov.au/GSWApublications

Cover image: Geologists in the field setting up seismometers for geophysical measurements

Contents

Scientific abstract.....	1
Lay abstract	1
Introduction.....	2
Principles of the Horizontal-to-Vertical Spectral Ratio (HVSr) passive seismic method.....	2
Study area	2
Basement geology	2
Cover context.....	3
Methodology	4
Selection of the study area.....	4
HVSr technique applied to the study of paleovalleys	4
Tromino seismometer technical details.....	5
Survey design in the southwest region of Western Australia	5
Acquisition settings	6
Results and data analysis	7
HVSr data quality	7
Velocity calibration at drillholes.....	8
Data visualization.....	10
Geological models	11
Discussion.....	17
Conclusions	21
Acknowledgements.....	21
References	21

Figures

1. Study area showing HVSr acquisition sites superimposed on regolith and MrVBF maps	3
2. Schematic HVSr spectral ratio data from a simple two-layer regolith–bedrock model	4
3. HVSr spectral plot displaying multiple frequency peaks detected by Tromino seismometers	6
4. Tromino 3G ENGy seismometer and three types of spikes	6
5. HVSr analysis in the proprietary Grilla software	7
6. An example of a broad frequency peak recording from Traverse S, site 37 (S37)	8
7. An example of a two-maxima stratigraphic peak recording from Traverse N, site 13 (N13)	9
8. Effects of noise removal – HVSr spectra and stability plots from Traverse S, site 18 (S18)	9
9. V_{s1} estimation at HVSr site M17DH	10
10. HVSr stations along S and M Traverses near the drillholes used for velocity modelling	11
11. Normalised HVSr values for all four traverses plotted in 3D	12
12. Data quality control at HVSr stations M05DH and M16DH using normalized values	13
13. Noisy HVSr recordings along Traverse C	14
14. Two velocity models over the study area	15
15. Example showing depth difference between the two velocity models	15
16. Profile view of the two velocity models against the drilling near Traverse S	16
17. Profile view of the two velocity models against the drilling south of Traverse C	16
18. Profile view of two velocity models 10 km southeast of Traverse M.....	17
19. Profile view of two velocity models near the HVSr recordings M16DH and M17DH	18
20. Plan view of three velocity models: a) hybrid; b) 520 m/s; c) 150 m/s	19
21. Profile view of three velocity models at three different locations for comparison	20

Table

1. Shear-wave velocity of various materials	5
---	---

Imaging the geometry of paleovalleys in the southwest region of Western Australia: linking basement and cover

S Jakica, P Duuring, I González-Álvarez¹ and JK Porter^{2,3}

Scientific abstract

The Horizontal-to-Vertical Spectral Ratio (HVSr) passive seismic method uses the natural resonance of the Earth to extract meaningful information about the subsurface structure. By analysing the ratio of horizontal and vertical ground motion spectral amplitudes, the HVSr technique can identify characteristic frequency peaks associated with the predominant subsurface layers.

This study demonstrates that regional-scale HVSr analysis can serve as an invaluable first-pass exercise for estimating the depth of paleovalleys. In this case the depth of the paleovalley marks the depth of the regolith cover above the potentially prospective basement, also termed here as depth-to-basement. The HVSr method's relative simplicity and cost-effectiveness makes it an attractive option, especially in regions with limited access to sophisticated geoscience data.

HVSr analysis of four traverses across the paleovalley in the southwest region of Western Australia generated three velocity models, with the third model, named here as the hybrid model, deemed optimal. All three models illustrate that the paleovalley's geometry closely conforms to the general topographic features of the current landscape. The hybrid model is a combination of the first two models. The hybrid model aligns favourably with drillhole data, demonstrating the consistency in the depth of the regolith cover, or paleovalley depth, estimates within the range of 0.4 to 10 m along the HVSr traverses. However, the study also notes the influence of implicit modelling and constrained HVSr data acquisition, which accentuates the disparity between the model and the actual drilling results as the distance from the traverse line increases.

While this approach provides valuable insight, a denser array of HVSr stations and further integration with other geophysical and geological information is recommended to refine and validate the basement depth or paleovalley geometry estimations.

KEYWORDS: mineral exploration, paleovalleys, passive seismic, southwest Yilgarn Craton, velocity model

Lay abstract

Common landscape forms in Western Australia's southwest include paleovalleys and paleochannels — ancient valleys and river systems filled with sand and gravel. These ancient waterways are key to understanding groundwater systems, placer gold deposits, and landscape evolution. To gain insights into their structure, this Report uses seismometers, geophysical tools that measure ground movements, to map the depth of these sandy terrains. This passive seismic method helps mapping the shape and size of the paleovalleys and paleochannels, aiding in our understanding of their geological and hydrological significance.

¹ CSIRO, ARRC, 26 Dick Perry Avenue, Kensington WA 6151

² Future Industries Institute, University of South Australia, Mawson Lakes, SA 5095

³ MinEx CRC, ARRC, 26 Dick Perry Avenue, Kensington WA 6151

Introduction

Non-invasive geophysical techniques provide a powerful tool in defining regolith sequences, including the thickness of the regolith cover. One such technique that has proven to be both useful and economic is the HVSR (horizontal-to-vertical spectral ratio) passive seismic method. HVSR passive seismic is a rapid, cost effective and non-invasive technique for estimating cover thickness. Globally, it has been successfully applied to estimate the regolith thickness in different regolith environments and geological settings (Delgado et al., 2000; Asten, 2004; Scheib et al., 2016; Kumar et al., 2018). HVSR has also been used to map the thickness of glacial sediments (Lane et al., 2008), and the geometry of paleovalleys and paleochannels (Jakica et al., 2021; Owers, 2016).

The objective of this study was to determine the effectiveness of deploying Tromino seismometers over a four-day period to acquire HVSR passive seismic data and interpret depth-to-basement variations in a study area located in the southwest region of Western Australia. In this study, the depth-to-basement marks the depth of the paleovalley. The study aimed to assess if such a rapid, cost-effective program could provide meaningful results in flat-lying areas with limited ground access (in this case, working in the agricultural region where field work is limited to the public ground only) and encourage the use of this technique in other parts of Western Australia. The study area was selected based on its prominent kilometre-scale drainage patterns with branching channels flowing towards the southeast. The study area also lies in the region prospective for minerals such as gold, iron and clay deposits. Consequently, an improved understanding of the cover characteristics in the region is of potential significance for mineral exploration.

This Report outlines the general principles of the HVSR method and its application to interpreting depth-to-basement measurements in paleovalley settings. The methodology used in this study is described in terms of planning traverses, deploying Tromino seismometers and collecting HVSR data. The results and data analysis section outlines the steps taken to process the raw data and validate the results against geological information obtained from existing drillholes in the area.

The discussion presents geological models for depth-to-basement in the study area based on the interpretation of HVSR and drillhole data. The conclusions include recommendations for improving geological models in the study area. Overall, the study demonstrates that the deployment of Tromino seismometers to acquire HVSR data is an effective and cost-efficient method for interpreting depth-to-basement variations in flat-lying areas with limited ground access. The study recommends further applications of this technique in other regions of Western Australia.

Principles of the Horizontal-to-Vertical Spectral Ratio (HVSR) passive seismic method

In contrast to active seismic methods, such as seismic reflection, which uses an artificial source such as a Vibroseis truck to excite a seismic response from the

subsurface, the HVSR method is a passive method that uses three-component measurements of ambient seismic energy, natural sound, to determine and evaluate a site's fundamental seismic resonant frequency (Nakamura, 1989; Lane et al., 2008). The resonant frequency is determined through analysis of the spectral ratio of the horizontal (north–south or X, east–west or Y) and vertical (up–down or Z) components of the ambient noise.

Originally developed to help define seismic hazards in Japan (Nakamura, 1989), the HVSR method is now broadly used across different industries such as resource exploration, the hydrogeological, geotechnical, and environmental sectors, as well as construction. In mineral and water exploration, the HVSR method is used to determine the depth to basement or other stratigraphic boundaries. The base of a paleochannel incised into basement is an excellent candidate for an HVSR passive seismic investigation (Scheib, 2014; Owers et al., 2016; Jakica et al., 2021). HVSR is a rapid and non-invasive method that measures ambient noise in the subsurface at the broad range of frequencies from 0.1 to 2048 Hz, over a set time interval (generally between five and sixty minutes). Signals above 1 Hz delineate shallow basement and/or intra-regolith interfaces. These signals are produced by microtremors, i.e. near-surface ambient vibrations from anthropogenic activity such as traffic, agriculture or industrial noise (Chandler and Lively, 2014; Meyers, 2017). Signals below 1 Hz are microseisms and are produced by natural forces, such as ocean waves, wind and deeper micro-seismic events (Chandler and Lively, 2014; Meyers, 2017). These signals usually delineate deeper regolith-to-basement interfaces (Meyers, 2017).

Study area

The study area is situated in the southwest region of Western Australia and includes a vast area extending from Katanning in the west to Hyden in the east, and from Gnowangerup in the south to Corrigin in the north (Fig. 1). The primary defining feature of the area is a paleovalley system, which may have contained a sprawling river drainage system in the past. The main channel, which is approximately 40 km wide, is in the northwestern part of the area near Corrigin (Fig. 1), and it divides into several second- and third-order channels that flow towards the southern coast of Western Australia in a southeasterly direction. Along the course of the drainage system, the mean elevation above sea level decreases from 430 to 190 m.

Basement geology

The basement rocks in the area include several narrow, discontinuous and irregularly shaped greenstone belts (Fig. 1). These belts are complexly deformed and consist of granulite-facies mafic and ultramafic rocks, siliciclastic and banded iron formation units (Gee et al., 1981; Gee et al., 1986; Myers, 1993; Wilde et al., 1996). They are enclosed by felsic gneiss and intruded by several generations of granitic intrusions. Additionally, hundreds of dolerite dykes, ranging from 1 to 100 m wide and less than 100 km long, cut these high-grade metamorphic and granitic rocks in an east–west and northwest–southeast direction (Quentin de Gromard et al., 2021). These dykes are undeformed and

unmetamorphosed. The main structural trend in the study area is towards the northwest, resulting from the alignment of greenstone belts, major northwest-trending regional faults, and dolerite dykes.

The Corrigin Tectonic Zone is a structurally complex domain that transects the study area (Fig. 1). This zone starts near Corrigin in the north and extends along a southeast strike to approximately 30 km east of Gnowangerup in the south. This is interpreted as the boundary between the younger basement rocks of the South West Terrane and the older rocks of the Youanmi Terrane to the east (Quentin de Gromard et al., 2021).

The study area contains several noteworthy mineralization occurrences as listed in MINEDEX. Among these is the Katanning gold trend that is located approximately 30 km east of the townsite and extends over a strike length of around 25 km in a northwest–southeast direction (Fig. 1). The greenstone belts in this region host gold deposits, including those in Katanning, Bottleneck, Griffins Find, Lake

Grace and Yandina. The gold mineralization in these areas is characterized by small gossans and soil anomalies that are rich in Au, Ag and Cu. Consequently, most drillholes in the study area are concentrated across these targets. Other mineralization prospects in the area include iron ore deposits, such as Kukerin Iron near Bottleneck and several occurrences located further north near Kulin. The area is also known for its clay deposits, such as Wickepin Kaolin, as well as past gypsum production in Lake Grace.

Cover context

The southwestern region of Western Australia is characterized by a regolith-dominated terrain, presenting unique complexities in its cover architecture. The part of this distinctive landscape where this study is conducted is situated at the boundary between two tectonic units: the southeast margin of the Yilgarn Craton and the Albany–Fraser Orogen (Fig. 1; e.g. Spaggiari et al., 2017).

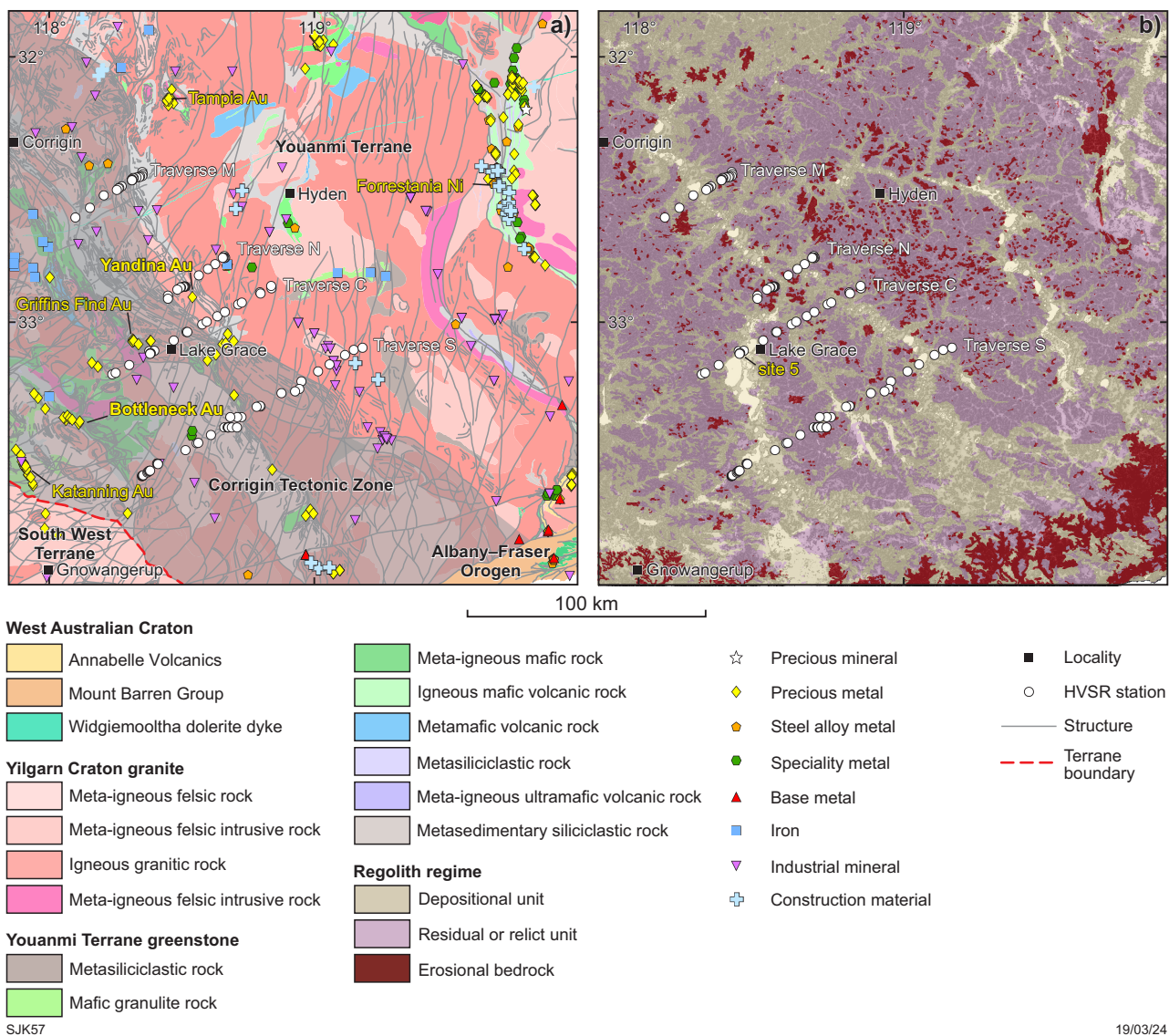


Figure 1. Study area showing four HVSR passive seismic traverses, including: a) a geological map overlain with mineral deposits and tectonic structures in the area (Quentin de Gromard et al., 2021); b) a regolith map superimposed on the MrVBF (Multi-Resolution Valley Bottom Flatness) map (de Souza Kovacs and Jakica, 2021; Gallant and Austin, 2011), featuring major localities

Within the study area, one can observe extensive paleovalley systems, as exemplified by Figure 1 (Commander, 1989; de Broekert and Sandiford, 2005). These paleovalleys, found in arid and semi-arid areas of Australia, exhibit drainage patterns that reflect the continental changes resulting from post-Mesozoic rifting and the northward drifting of Australia (Magee, 2009).

The dynamics of coastal sedimentation in the region are greatly influenced by sea-level changes, which occur in transgression–regression cycles. These cycles drive erosion and the redistribution of continental sediments along the changing shoreline. Notably, the southwestern coastline of Western Australia has experienced significant depositional events during the Paleocene–Quaternary period. These events are attributed to eustatic sea-level variations that inundated the Albany–Fraser Orogen and possibly parts of Yilgarn Craton, causing paleovalleys and paleodrainages to become submerged up to 400 km inland from the present coastline (Hou et al., 2008; González-Álvarez et al., 2016; Pernreiter et al., 2018).

The regolith that covers the southwestern region of Western Australia exhibits a complex profile. It encompasses weakly weathered bedrock, saprolite and a clay-rich zone, transitioning into an upper section that can be ferruginous, siliceous or bauxitic. This upper section is commonly overlain by varying thicknesses of sand and silt (e.g. Cornelius et al., 2007; Anand and Butt, 2010).

A salt-lake drainage system covers large portions of the study area, with rare outcrops of granitic rock and felsic gneiss locally preserved, with remnants of lateritic duricrust typically found on topographic high points. A study by de Souza Kovacs (2022) suggests that there is a spatial relationship between Au and Hg concentrations in laterites with deep crustal structures at the margins of greenstones and crustal domains in the central southwest Yilgarn Craton. The study further suggests that anomalous concentrations of Au and Hg in laterite also show a spatial relationship to neotectonism in the area (de Souza Kovacs, 2022).

Weathering depths constrained by mineral exploration drilling varies throughout the study area, for example in the Katanning area depth-to-basement contacts range from near-surface to 70 m in proximity to drainage features (Tyrer, 1980).

Methodology

Selection of the study area

The southwest region of Western Australia presents a perfect case study for testing the utility of the HVSR method in mapping wide paleovalleys. This study was designed to intersect various geological and regolith settings, with the objective of providing constraints on the depth of cover in this area. It is important to note that this study tests only one method and intentionally lacks integration with multiple independent datasets (e.g. comprehensive closely spaced drilling, airborne electromagnetic surveys). Therefore, it is designed to establish the limits of this method as a standalone, first-pass approach that could be beneficial during the early phases of regional exploration.

HVSR technique applied to the study of paleovalleys

The HVSR method is based on a simple two-layer system, such as regolith cover overlying bedrock. The resonant frequency is amplified with a stronger and sharper impedance contrast between the two units (Fig. 2). A very strong impedance contrast is generally observed at the regolith–bedrock boundary due to vastly different properties of the crystalline basement and overlying, less consolidated regolith material. The shear impedance contrast results from the different shear-wave velocities (V_{s1} , V_{s2}) of the two layers and their respective densities (Fig. 2). The shear-wave velocity is a measure of how fast seismic shear waves travel through a rock unit. Some examples of shear-wave velocities for different materials, ranging from soft soils to hard rock, are listed in Table 1. The greater the difference in shear-wave velocity between the two units, the larger the impedance contrast, and the greater the resonant frequency peak in HVSR. The resonant frequency (f_z) at which the impedance contrast is measured is a function of the depth of the boundary between the two units (Fig. 2):

$$f_z = V_{s1} / 4h_1 \quad (\text{Equation 1})$$

The relationship between the frequency (f_z), shear-wave velocity of the unit in question (V_{s1} ; Fig. 2) and the thickness of the unit (h_1 ; Fig. 2) is the basis of the short-station passive seismic approach to estimating cover thickness. In this study, the resonant frequency peak produced by an impedance contrast at depth is also referred to as a stratigraphic peak. Frequency peaks produced by uncorrelated noise, for example wind, are referred to as non-stratigraphic peaks.

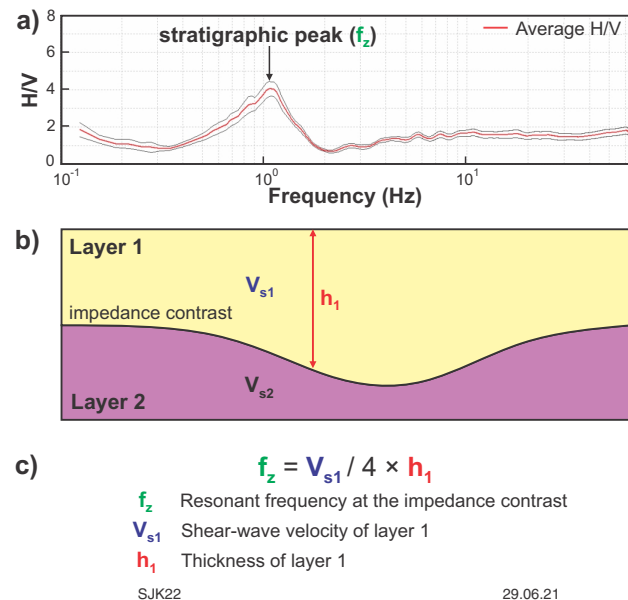


Figure 2. Schematic HVSR spectral ratio data from a simple two-layer regolith–bedrock model: a) H/V spectral ratio plot with a peak at the resonant frequency (f_z) indicating an impedance contrast at depth; b) simple two-layer regolith–bedrock model with an impedance contrast at depth (h_1); c) Equation 1 showing the relationship between the resonant frequency, shear-wave velocity (V_{s1}) and depth to the impedance contrast (h_1)

Table 1. Shear-wave velocity of various materials

Material	V_s (m/s)	Source
Clay, tuffs	180	Micromed, 2009; Ibs-von Seht and Wohlenberg, 1999
Clay and sandy silt	200	Micromed, 2009; Ibs-von Seht and Wohlenberg, 1999
Sand and gravel	300	Micromed, 2009; Ibs-von Seht and Wohlenberg, 1999
Gravel and altered/soft rock	400	Micromed, 2009; Ibs-von Seht and Wohlenberg, 1999
Soft/layered sedimentary rock	500	Micromed, 2009; Ibs-von Seht and Wohlenberg, 1999
Alluvium (at 30 m depth)	257–338	Collins et al., 2006
Archean granite (in WA, at 30 m depth)	>750	Scheib, 2014
Hard rock	>1500	Scheib, 2014; Ibs-von Seht and Wohlenberg, 1999

There are some limitations to using the HVSR technique that must be considered when interpreting results or designing surveys. If the overlying and underlying units have similar petrophysical properties, or there is a gradational contact between units, the resulting weakened impedance contrast means that the resonant frequency, and hence the HVSR peak, are poorly defined (SESAME European Research Project, 2004; Lane et al., 2008). For example, while mapping the thickness of till units in Northern America, Lane et al. (2008) found that a low impedance contrast between the till and deeply weathered bedrock resulted in a poorly defined HVSR peak. In areas characterized by deep weathering, a poorly defined HVSR peak might be produced by a gradational increase in velocity and reduced impedance contrast at the regolith–basement interface. In such environments, it is recommended to obtain a good coupling of the instrument with the ground by digging a shallow hole and placing the instrument in the hole. This reduces the chance of uncorrelated surficial noise further masking the HVSR reading (Feldpausch, 2017). Further, the visualization of masked signals can be amplified by normalization during data processing (see **Data visualization** section below for further details).

Tromino seismometer technical details

The instruments used to acquire HVSR data in this study were Tromino seismometers. The Tromino is a three-component seismometer that measures ambient seismic noise in the subsurface in the range of frequency of 0.1 to 200 Hz (MoHo, 2017). Each instrument has three orthogonal electrodynamic velocimeters with selectable gain for seismic tremor acquisition (MoHo, 2017). The acquired data are stored in an internal memory card and transferred to a PC using Grilla v. 9.7 proprietary software provided by MoHo Science and Technology.

The Tromino instrument can detect multiple frequency peaks where there are strong impedance contrasts between layers. Peaks occur at the resonant frequency corresponding to each layer, with deeper impedance contrasts producing lower frequency peaks (Fig. 3).

Survey design in the southwest region of Western Australia

This study utilized 23 short-station seismic HVSR Tromino 3G energy seismometers to investigate paleovalley mapping in the southwest region of Western Australia. The study was supported by 19 Tromino devices owned by CSIRO (Commonwealth Scientific and Industrial Research Organisation) and four instruments that belong to the GSWA (Geological Survey of Western Australia). Due to restricted access to private farmlands in the area, the seismometers were deployed in selected public spaces, mostly along the margins of paved or unpaved roads (Fig. 1).

Ninety-seven stations were deployed along four traverses running in a general southwest–northeast direction (Fig. 1). The traverses were designed to cut across the northwest–southeast-trending paleovalleys of the study area. A digital elevation Shuttle Radar Topography Mission 1 arc second (SRTM 1) and Multi-resolution Valley Bottom Flatness (MrVBF) models were used for selecting the location of traverses (USGS, 2014; Gallant and Austin, 2011). Shorter (32–35 km long) traverses were planned in the northwestern areas of the study area where main drainage channels are present, whereas longer (70–100 km) traverses were designed in southeastern areas due to the branching of the drainage system into multiple second- and third-order channels (Fig. 1). The spacing between the traverses, and the HVSR stations along them, depended upon the geometry of the drainage system and the best road access sites.

The focus of the survey design was to test topographically low and high areas of the paleovalley in order to determine correlation of cover thickness. Special attention was paid to the drillhole distribution in the area. Drilling information was used to obtain subsurface velocities during the processing phase by comparing logged depth intervals of cover–basement contacts to the nearby collected seismic data. The positions of stations were also selected to cover diverse regolith and geological settings across the paleovalleys.

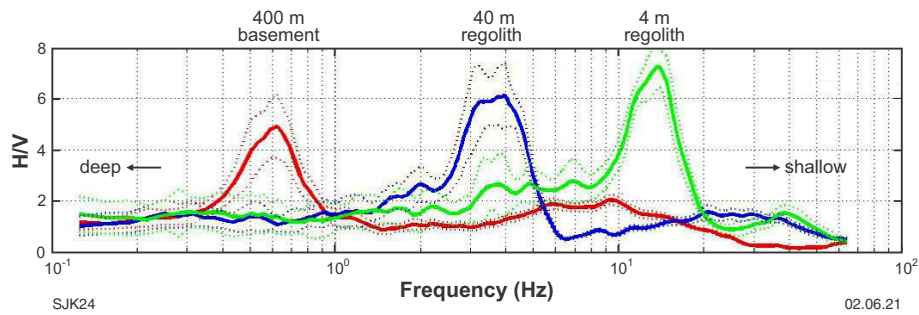


Figure 3. HVSR spectral plot displaying multiple frequency peaks detected by Tromino seismometers (adapted from MoHo, 2017). In this example, lower frequency peaks signify the deeper basement interface, while higher frequency peaks correspond to shallower intraregolith interfaces

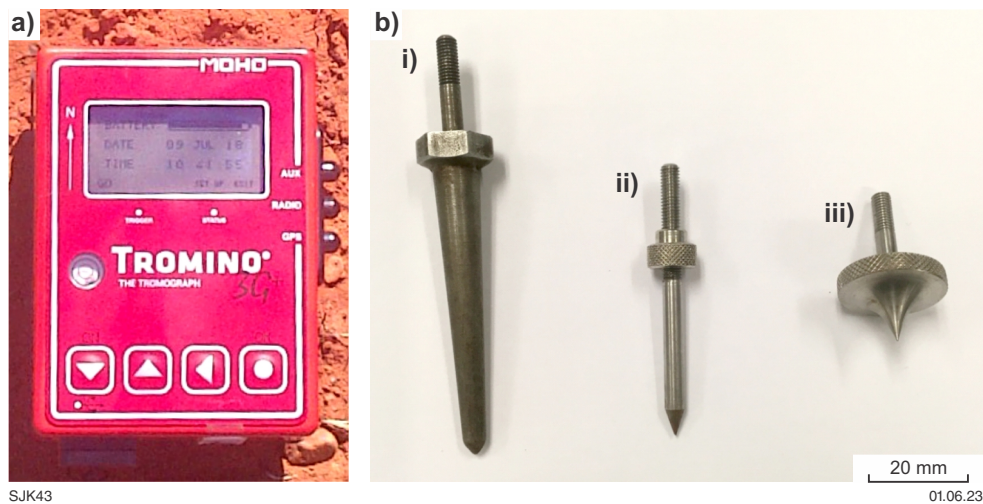


Figure 4. Tromino 3G ENG seismometer: a) Tromino seismometer; b) spikes for ground coupling (i, custom-made, 10 cm total length and 6-cm penetration length; ii, long spike, 6 cm total length and 4-cm penetration length; iii, short spike, 3 cm total length)

Acquisition settings

At each Tromino deployment site located along a public road, a 1 m² area of ground was selected that was level and clear of vegetation and located as far as possible from the road (usually 2–5 m from the edge of the road). Most sites were along infrequently used unsealed roads, with only a few instrument deployments on the side of busy highways. Ground conditions varied among the 97 collection sites, including soft soil, sandy lateritic soil, gravel road, organic clay-rich soil, muddy sand, and hard, consolidated sand. In most environments, it was possible to select patches of ground with firm support; however, in areas of salt lakes it was not possible to find ideal areas, so Tromino measurements were performed on soft, muddy soils along the margins of the lake. To ensure good coupling with the ground and optimal signal transfer, three spikes were mounted into each Tromino seismometer, which was then pushed evenly and firmly into the ground until the ground resisted full penetration of the spikes (Fig. 4a).

This study used three different types of spike (Fig. 4b), dependent on the ground conditions, to ensure good ground coupling: 6 cm-long spikes with 4-cm penetration length; short, round spikes (3 cm total length) and custom-made conical spikes that are 10 cm long with a 6-cm penetration length. The long and short spikes came as standard equipment with the instruments from the manufacturer.

The custom-made spikes were designed by the Centre for Exploration Geophysics, WA School of Mines, Curtin University, for better coupling. Their conical design resembles spikes that are used for conventional reflection seismic geophones.

Each long-axis side of the rectangular Tromino instrument was oriented parallel to magnetic north and the levelling spirit bubble was used to ensure the device was horizontal. At the time of the survey, the declination of the magnetic grid to true north was insignificant (0.8 degrees) and hence no correction to true north was necessary (determined by referring to the Geoscience Australia website, <<https://geomagnetism.ga.gov.au/main>>, accessed May 2022).

After an initial 15 second delay, to enable the worker to leave the site vicinity, HVSR readings were collected over a 20-minute recording period. The most efficient method for Tromino deployment and communication was the operation of two field vehicles, starting the deployment at opposite ends of the traverse line, moving towards each other and meeting near the middle of the traverse. Each vehicle operated with two team members that performed complementary duties. One team member navigated and was responsible for deployment of the Tromino instrument, while the second member drove and recorded site information (such as exact location, time and ground conditions for each site). Over the four days of data

collection, taking place in mid-May 2022, no rain influenced the survey, although wind conditions were moderate at times. In most cases, the Tromino instruments benefitted from being positioned in the leeward side of natural obstacles (plants, sand piles, rocks) and were therefore less affected by wind. A research team usually deployed up to 10 Tromino devices in sequence along the traverse. After waiting for the 20 minutes of collection time at the last site, the deployed instruments were rapidly collected by navigating backwards to each existing site. The entire procedure was then repeated until meeting the second team near the middle of the traverse. Acquired data were downloaded at the end of each day and rapid in-field quality control was performed to ensure completion of the traverse had been achieved.

Results and data analysis

HVSR data quality

After downloading the data using MoHo's proprietary Grilla software, individual measurements were selected for analysis. It was observed that the recordings from the deepest part of the paleochannel had the most distinct HVSR peaks. An example of such a recording is presented in Figure 5. The example shows results from Traverse C, site 5

(refer to Fig.1 for location of traverses). The recording shows an acquired HVSR spectral ratio (red line) and the 95% confidence limits (grey lines; Fig. 5a). The stratigraphic peak occurs at 1.09 Hz, which being close to 1 Hz, indicates an impedance contrast at depth rather than a shallow regolith interface or cultural noise effect. The amplitude spectra of the three components were computed for each 20-second window via fast Fourier transformation and smoothed with a triangular 10% window (Fig. 5b).

Horizontal components – north–south (green) and east–west (blue) – in the amplitude spectra are usually very similar unless there is strong anisotropy in the near surface. The vertical (purple) component dips due to resonance from trapping by underlying layers, creating an eye-like shape in the amplitude spectra (Fig. 5b). This eye-like shape in the amplitude spectra corresponds to the stratigraphic peak in the HVSR data (Fig. 5a). The consistency of the noise signal throughout the acquisition is shown in the time stability plot (Fig. 5c). A linear feature in the stability plot represents a constant, coherent noise occurring at the same frequency as the eye-like shape in the amplitude spectra and the stratigraphy peak in the HVSR data and, in this report, is referred to as the normal trend.

At some sites, broad frequency peaks were measured (Fig. 6). Such recordings have been processed with caution and their interpreted depths are less reliable.

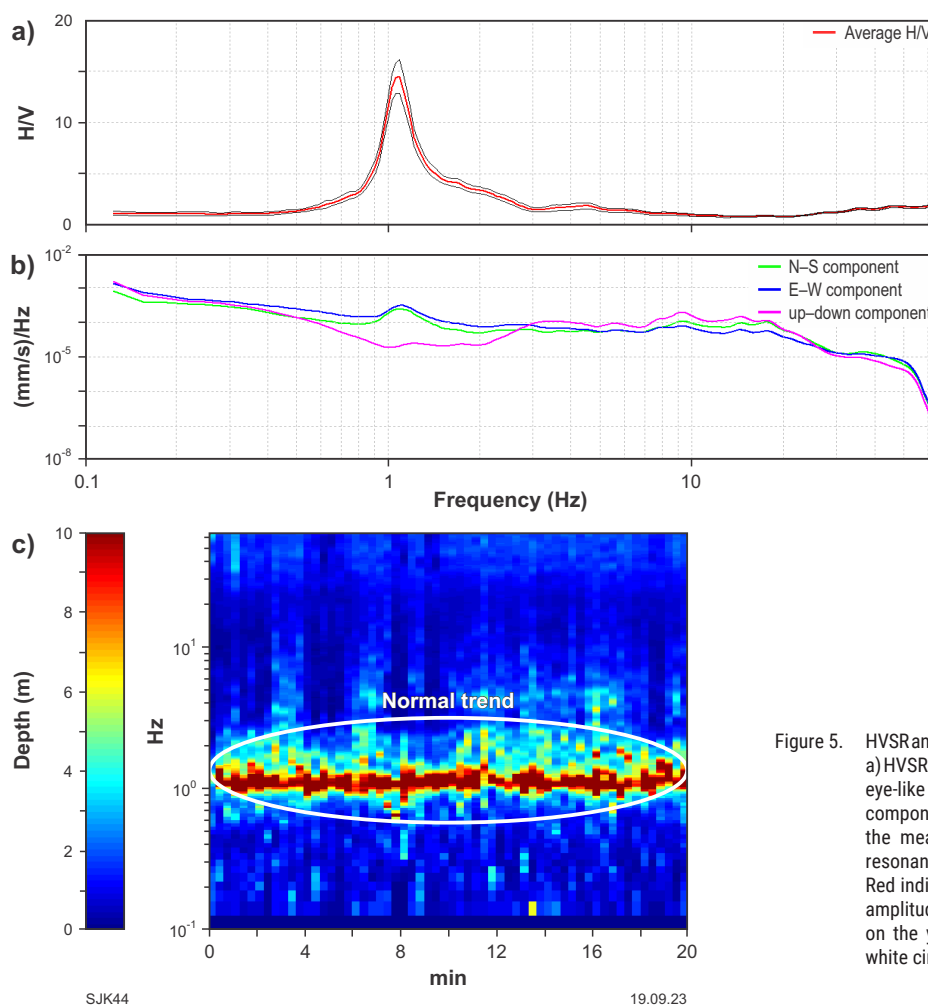


Figure 5. HVSR analysis in the proprietary Grilla software, including: a) HVSR spectra; b) amplitude spectra displaying distinct eye-like shapes formed by the horizontal and vertical components; c) stability plot of the HVSR curve during the measurement, illustrating the amplitude of the resonant frequency over a 20 minute acquisition period. Red indicates high amplitude, while blue indicates low amplitude. Time is plotted on the x-axis, and frequency on the y-axis. The normal trend is represented by a white circle

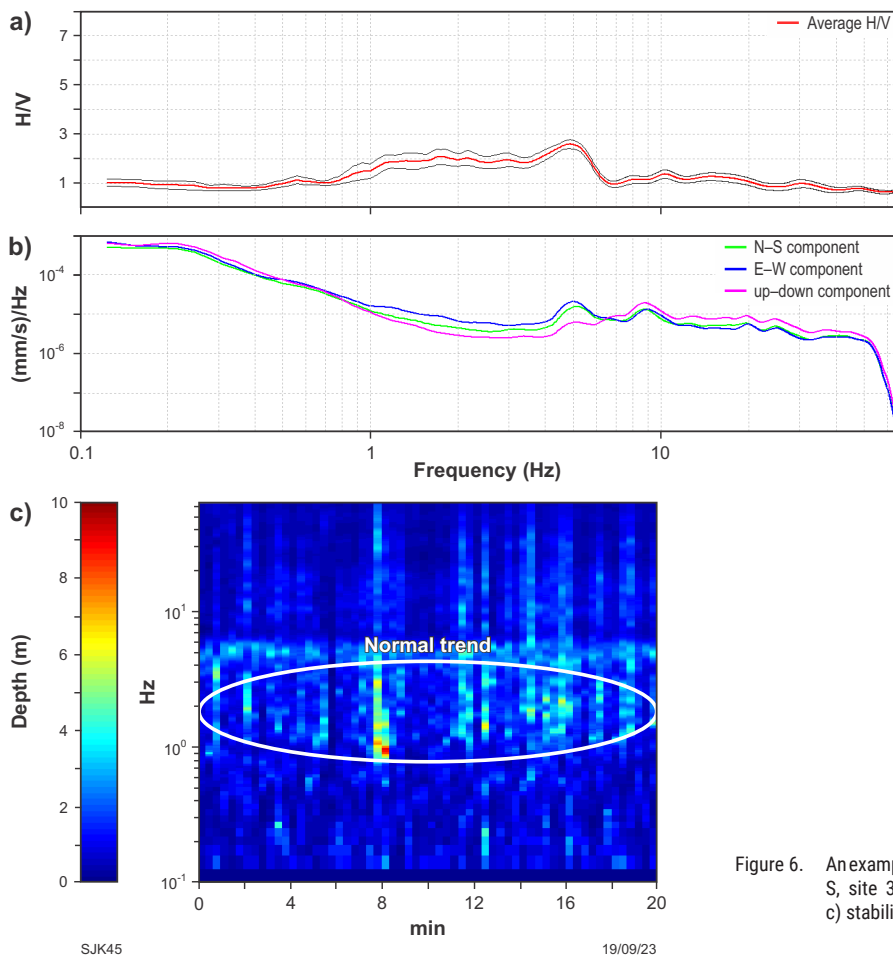


Figure 6. An example of a broad frequency peak recording from Traverse S, site 37 (S37): a) HVSR spectra; b) amplitude spectra; c) stability plot

At several sites, stratigraphic peaks with two maxima were observed in HVSR spectra (e.g. Traverse N, site 13; Fig. 7). The two maxima possibly indicate a thin layer of material, such as weathered bedrock, at the regolith–bedrock interface. At such sites, both peaks were modelled and checked against the HVSR recording near that site, as well as against other available data, such as regolith and geology maps. The peak whose recording was in better agreement with other data was then chosen as a preferable peak for the model.

Transient and/or near-white noise (e.g. nearby livestock, passing traffic, wind, or other acoustic noise) was recognized by a signal that strongly deviated from the normal trend. Transient noise appears as dispersed warm colours in the stability plot (Fig. 8). Sometimes the data quality was improved by removing the noise from the readings (Fig. 8b). An HVSR stability plot before noise removal is presented in Figure 8a, where the normal trend is a maximum HVSR of 4 Hz, while the noisy windows show dispersed warm colours away from the normal trend at lower frequencies. The noisy data were excluded from the analysis by selecting only certain windows of data, as demonstrated in Figure 8b.

Six recordings were faulty, or masked by high-amplitude transient noise that could not be removed. Two of these six recordings had a nonresponsive Z component, which may have been due to poor coupling in moist ground conditions. The other four recordings were masked by high amplitude noise. All six recordings were discarded from further processing.

Velocity calibration at drillholes

Interpretation of HVSR measurements using Grilla software involves fitting a synthetic curve to the measured frequency peaks in the HVSR spectrum (Fig. 9). This was carried out by constraining a velocity–depth model using Equation 1 and HVSR readings collected close to drillholes located along Traverses S and M. Along Traverse S, the velocity constraint was performed based on the following HVSR readings and their proximity to the drilling information where depth to basement was known. HVSR readings S16–S18 are within 3 km of five Magnetic Resources drillholes (RDC-1-5; mentioned within the WAMEX ‘A number’ report A90754), while HVSR readings S22–S24 are within 600 m of 23 Dominion Mining Limited drillholes (04YVR043–04YAC065 documented within the A78275 report) (Fig. 10a) (Hirschmann, 2008; Reddy, 2011). HVSR readings used for velocity constraints along Traverse M include drillholes M09 and M16DH–M18DH, which are located within 30–570 m of Cygnus Gold Limited and North Limited drillholes (Fig. 10b) (see A123856 and A56202 reports, respectively; Sowerby and Mills, 1998). All drilling information, with reports, geology information and collars can be downloaded for free from the GSWA data portals, GeoVIEW.WA and GeoDocs. The modelled velocities of 520 m/s for Traverse S and 150 m/s for Traverse M were used at each subsequent HVSR measurement to estimate the depth to basement.

A limitation of this study is that the shear-wave velocity of the regolith package has only been calculated using drillholes along two of the four traverses, and some drillholes were up to 3 km from an actual HVSR reading.

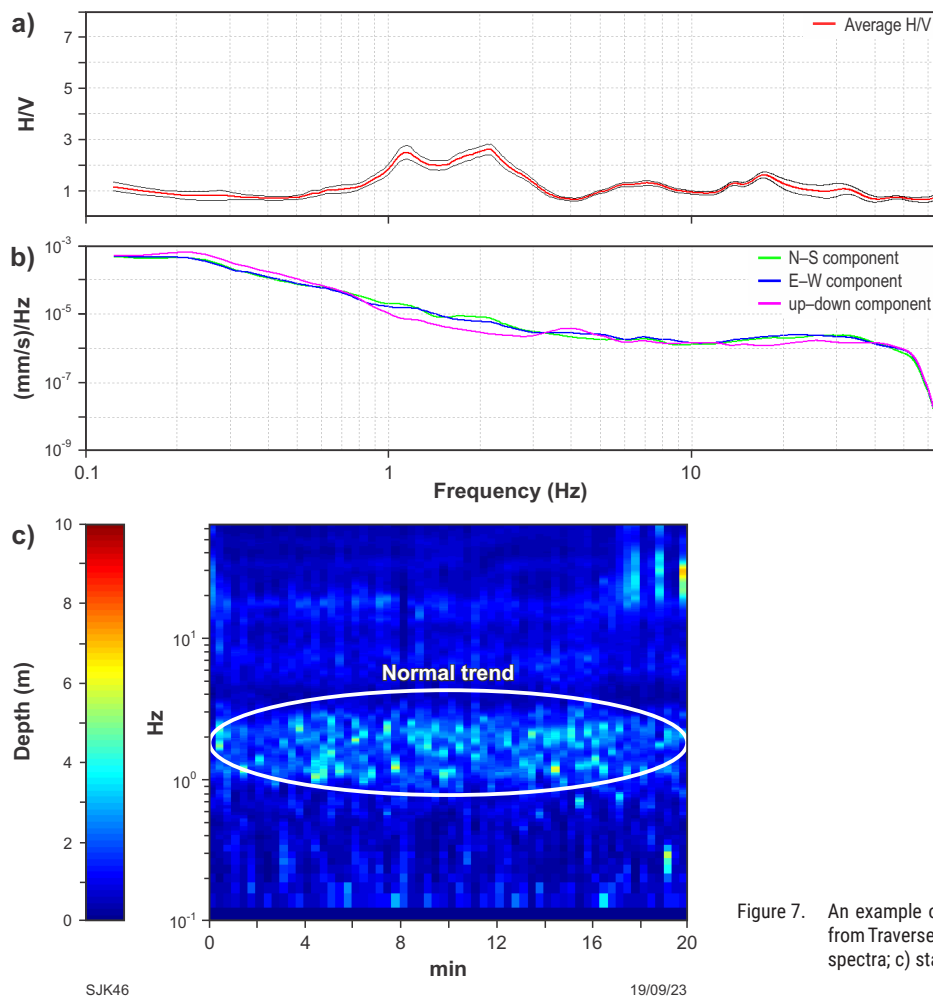


Figure 7. An example of a two-maxima stratigraphic peak recording from Traverse N, site 13 (N13): a) HVSr spectra; b) amplitude spectra; c) stability plot

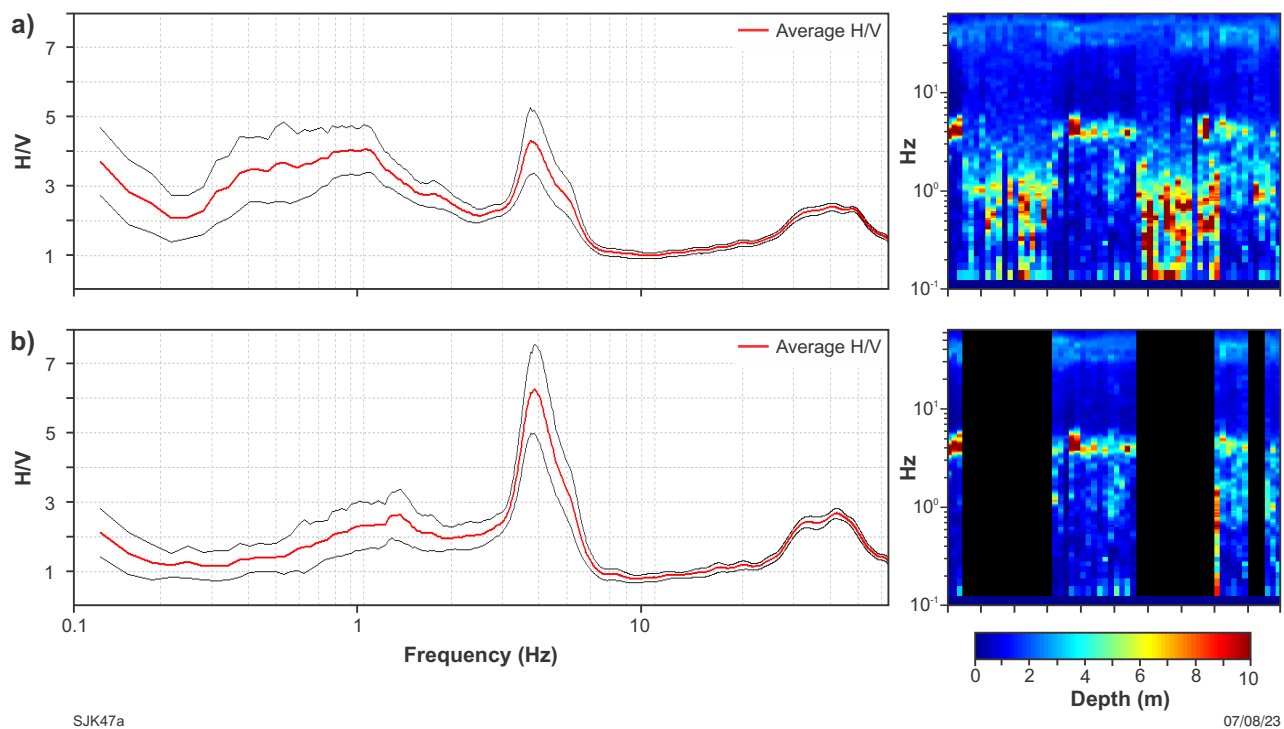


Figure 8. Effects of noise removal – HVSr spectra and stability plots from Traverse S, site 18 (S18): a) before; b) after trace cleaning

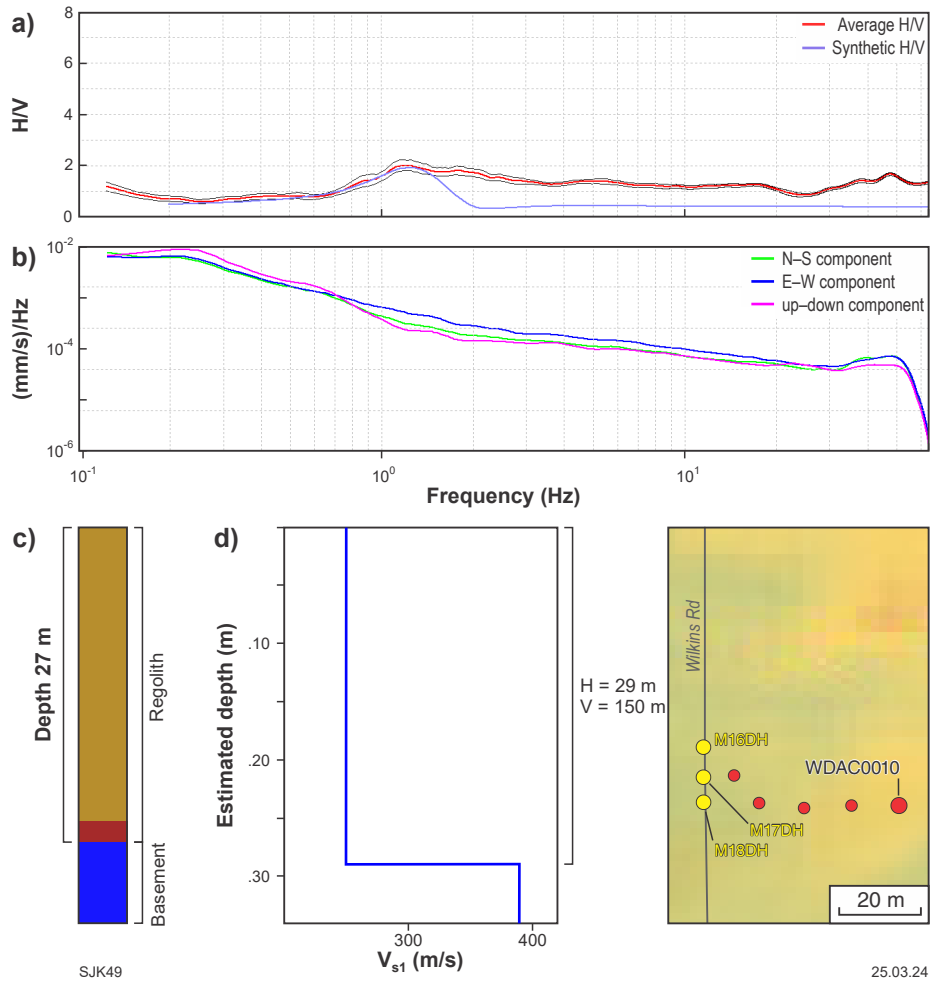


Figure 9. V_{s1} estimation at HVSR site M17DH, including: a) observed (red and black) and synthetic (blue) H/V spectra; b) amplitude spectra; c) logged geology at drillhole WDAC0010, located less than 100 m from the HVSR reading; d) velocity model and associated parameters, including the V_{s1} used to generate the synthetic H/V spectra in a)

In addition, the accuracy of existing drillhole logs is uncertain in some cases. For example, drillhole WDAC0006, located 35 m east of HVSR site M16DH, has weathered rock documented above and below an unweathered rock interval at 6–12 m depth. Such a relationship, while geologically permissive, complicates the simplified placement of a single cover–basement contact interpretation for this drillhole, which is then extrapolated for the region. The study used what seemed to be the most reliable and accurate drillhole logging. No drillholes that reach the basement were publicly available along Traverses C and N. The use of this constant velocity throughout the study area is a simplification, but without more basement-intersecting holes, this approach is unavoidable.

Data visualization

To visualize HVSR data, HVSR values have been normalized and frequencies converted to elevations. HVSR values at each site have been normalized using the min.–max. normalization formula:

$$x^1 = (x - \min(x)) / (\max(x) - \min(x))$$

where: x^1 = normalized value
 x = original value

Normalization transforms the HVSR amplitudes, which can vary significantly between sites, to a range between 0 and 1. This makes the HVSR values comparable between sites, although in some cases enhances noise.

Measured frequencies were then converted to elevations. These frequencies (f_z) were converted to thickness (h), assuming a velocity (V_s) of 520 m/s or 150 m/s and using the equation $f_z = (V_s/4h)$. The calculated thickness was then subtracted from the elevation of the site to give the depth of that data point (corresponding to the vertical depth to basement). To conform with other data, the elevation of the SRTM 1 image was used for each HVSR recording (USGS, 2014). SRTM 1 is digital elevation data at a resolution of 1 arc-second or approximately 30 metres. Normalized HVSR values for the four traverses are shown in Figure 11.

The normalized images were mostly used to check data quality before modelling the depth to basement. For example, along traverse M, the HVSR spectral plot from recordings at stations M16DH and M05DH displayed double peaks (Fig. 12). When viewed in the 3D Leapfrog Geo software as normalized data, it was easy to recognize that the lower-frequency peak aligned with the rest of the model, and hence those peaks were chosen for the final model (Fig. 12). Furthermore, after analysing the normalized

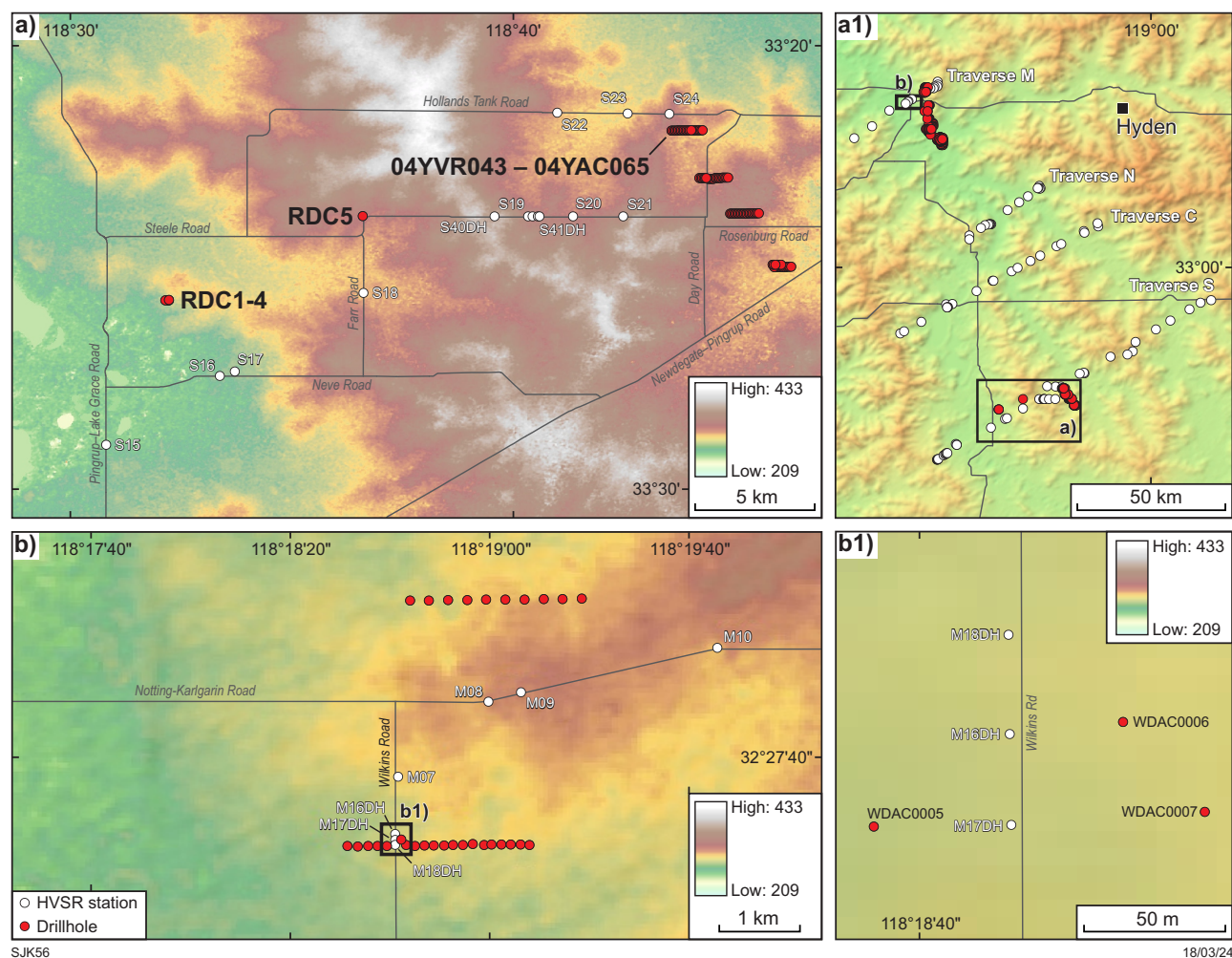


Figure 10. HVSR traverses showing: a) HVSR readings along Traverse S near the drillholes used for the velocity model; a1) zoomed out map for location purposes; b) HVSR readings along Traverse M near drillholes used for the velocity model; b1) inset showing the location of HVSR recording stations and drilling. The DEM image used for this figure is an SRTM 1 image (USGS, 2014)

data, HVSR recordings for stations C20DH, C21DH and C04 (along Traverse C) all showed false readings (Fig. 13). These recordings were then double-checked in the raw HVSR data, where it was confirmed that the data were too noisy for interpretation (Fig. 13). As a result, these three recordings were removed from the geological models.

Geological models

Two velocity models (520 m/s and 150 m/s) were generated from the HVSR passive seismic data (Fig. 14a,b), and the results were converted to depths. Both models were generated based on the drilling information in the vicinity of the HVSR traverses. Both models show similar paleovalley geometry. Despite the scarcity of data, the depth-to-basement models agree with the current surface valley geometry (Fig. 14c). Cross-sectional views show that although both models map the overall geometry of the paleovalley, their depths are significantly different, where the depth difference between the two models reaches up to 53 m (Fig. 15). In the southern part of the study area, the 520 m/s velocity model displays a better match with drilling in that area (Fig. 16).

The modelled depth to the basement is within 0.4 to 10 m accuracy when compared with the drilling data (Fig. 16), while the 150 m/s model is shallower and not in concordance with the basement depths intersected by drilling (up to 45 m discrepancy). The same is observed to the south of the southwestern part of Traverse C, and ~10 km southeast from the northeastern part of Traverse M, where the 520 m/s model is in better agreement with drillhole data (Figs 17 and 18, respectively).

Figure 17 shows that the 520 m/s velocity model has 3 to ~15 m discrepancy with the drilling data, while the 150 m/s model shows over 30 m discrepancy at all drillholes (see WAMEX reports A90254 and A117455) (Tolson, 2011; Gasson, 2018). Figure 18 illustrates that the 520 m/s velocity model is within 10 m accuracy with the basement depth mapped by the drillhole KDA9 (see WAMEX report A56202; Sowerby and Mills, 1998). Conversely, the 150 m/s model shows approximately 53 m discrepancy (Figure 18). The only example where the 150 m/s model takes precedence over the 520 m/s model is near the drillholes close to HVSR stations M16DH and M17DH (Figs 10, 19). At this location, the 520 m/s model is more than 500 m deeper than the basement depth recorded by drilling in the area, while the 150 m/s model is within 2 to 12 m accuracy of the drilling data (Fig. 19) (see GSWA WAMEX A123856 report; Cherry, 2020).

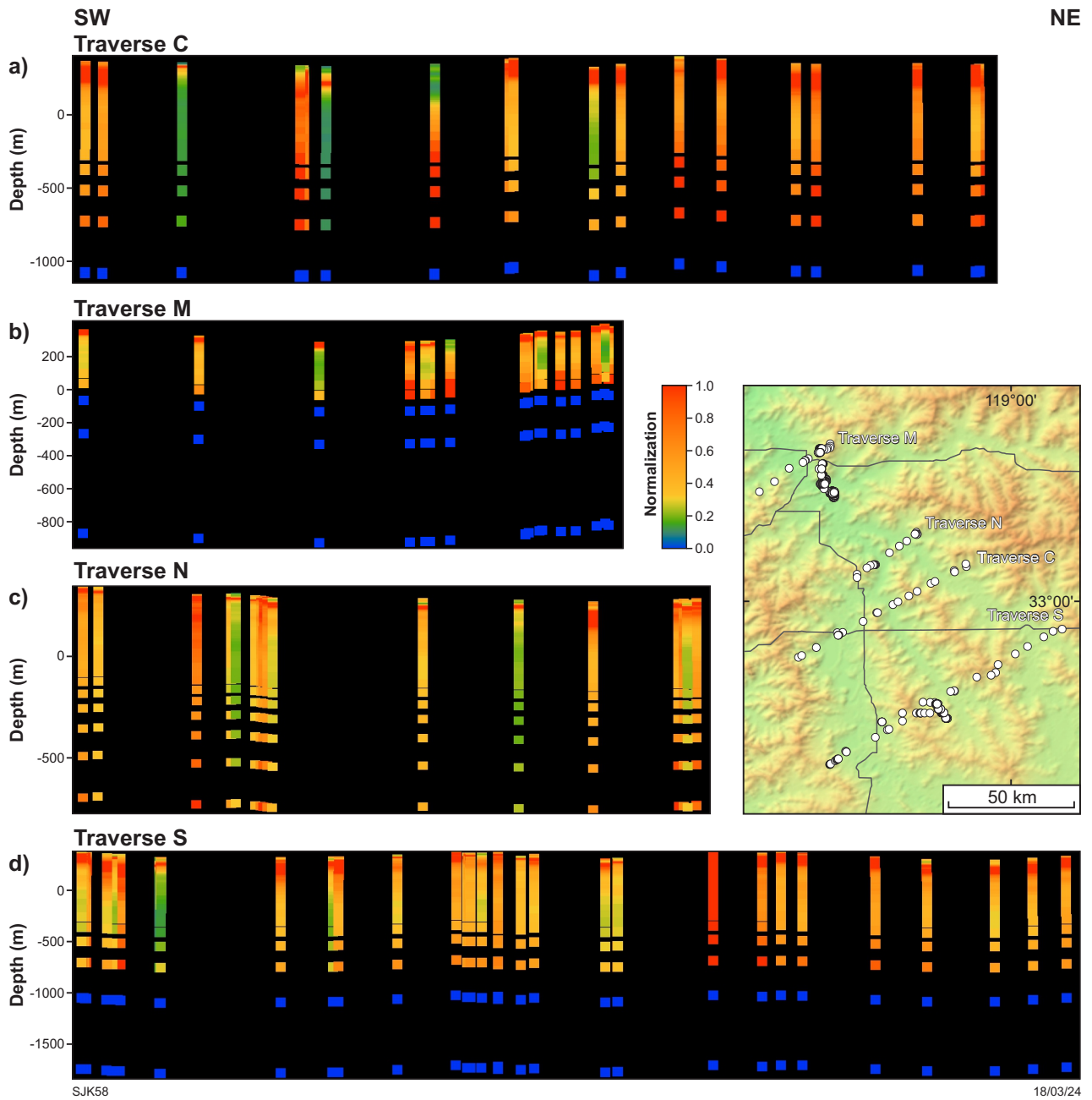


Figure 11. Normalized HVSR values for all four traverses plotted in 3D: a) Traverse C; b) Traverse M; c) Traverse N; d) Traverse S

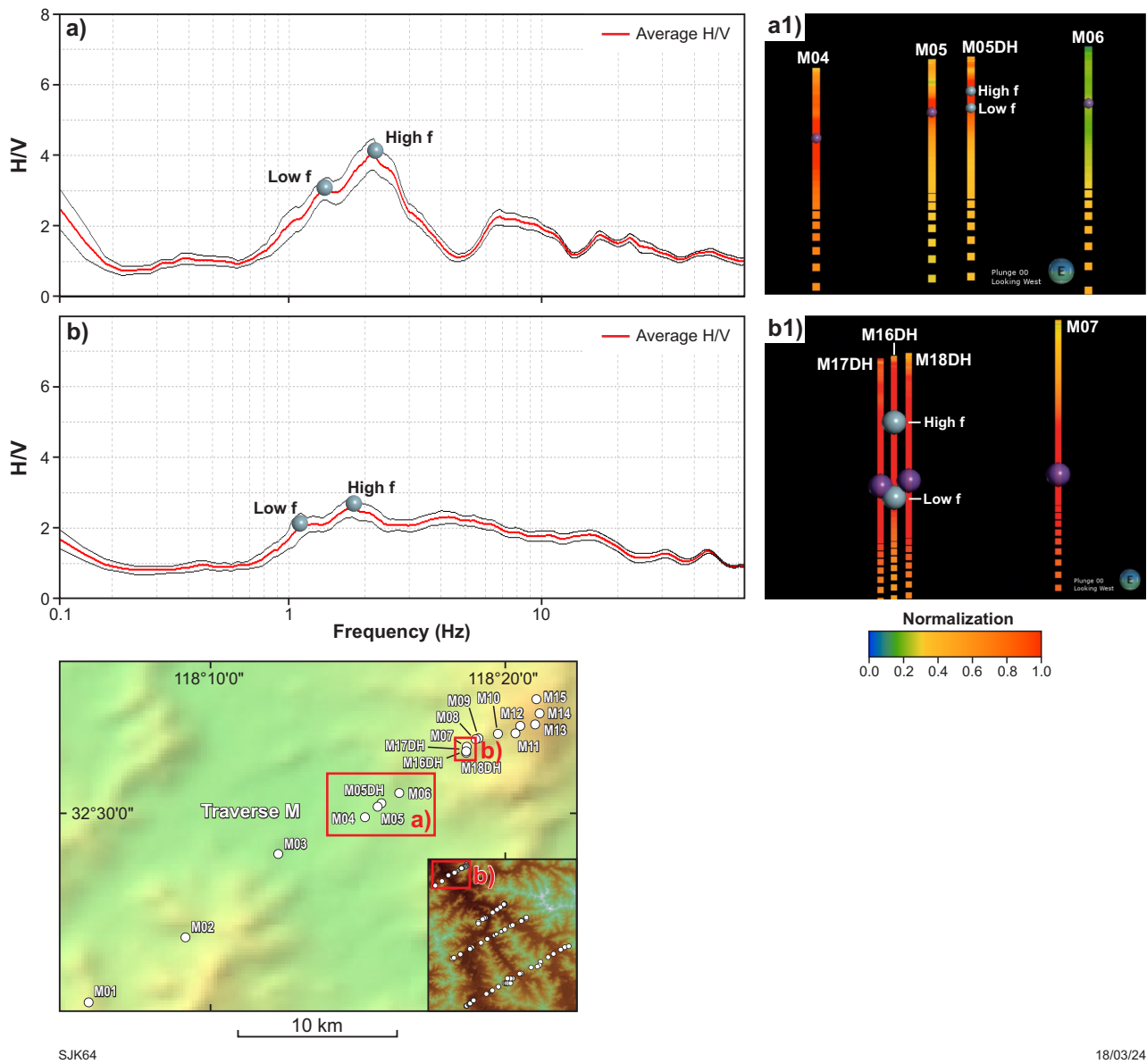


Figure 12. Data quality control using normalized images. This example demonstrates quality control at stations M05DH and M16DH, where double peaks were observed in the HVSr spectral plot: a) double-frequency peak observed in the M05DH HVSr recording, showing both low-frequency and high-frequency peaks; a1) comparison of both frequency peaks at station M05DH (grey circles) with frequency peaks at neighbouring stations (indicated by purple circles); b) double-frequency peak observed in the M16DH HVSr recording, showing both low-frequency and high-frequency peaks; b1) comparison of both frequency peaks at station M16DH (grey circles) with frequency peaks at neighbouring stations (indicated by purple circles)

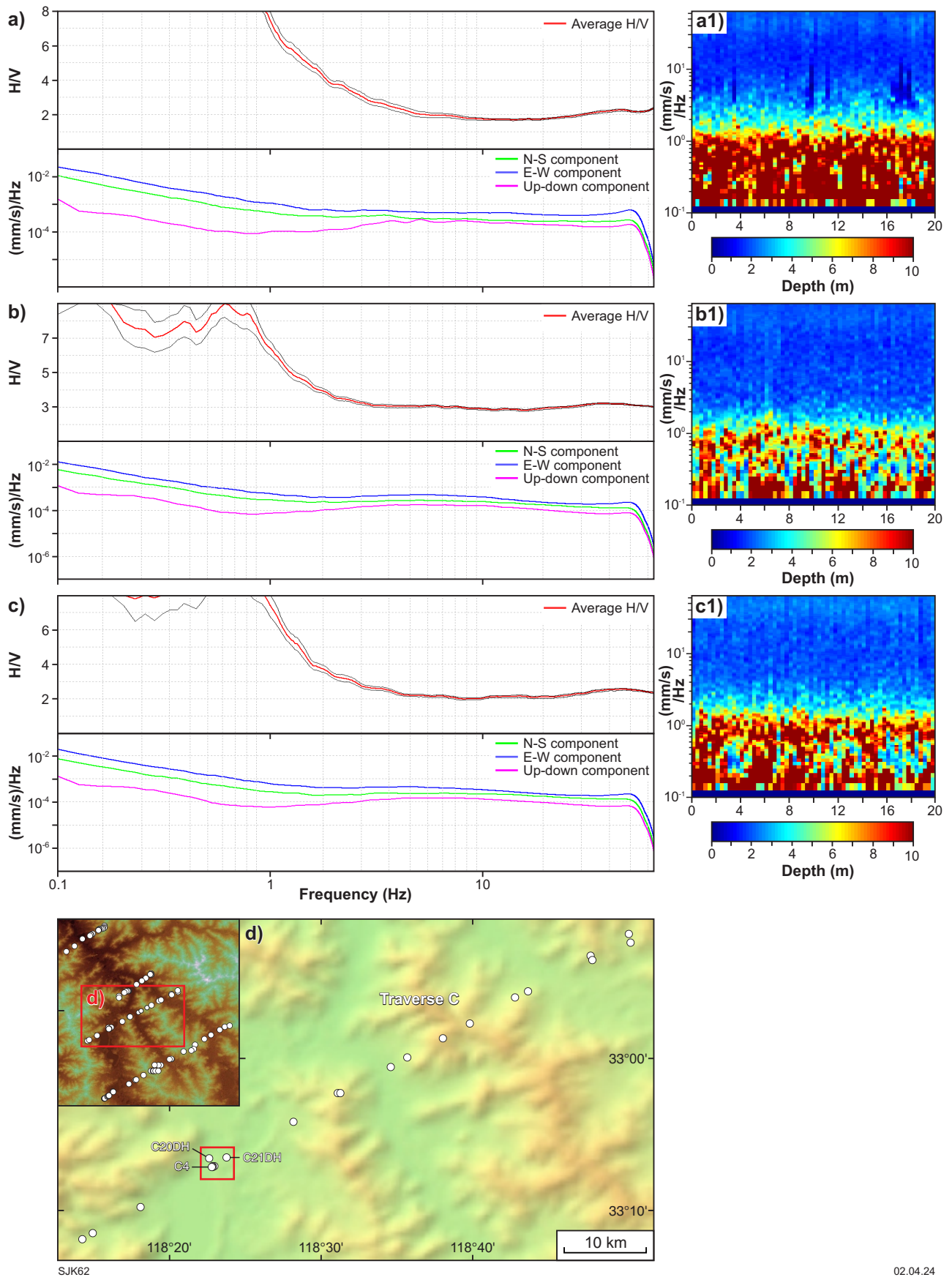


Figure 13. Three noisy HVSR recordings along Traverse C: a) C20DH; b) C21DH; c) C04; d) locality map. These recordings have been removed from the model. Images a1, b1 and c1 illustrate large increases in noise at frequencies below 1 Hz

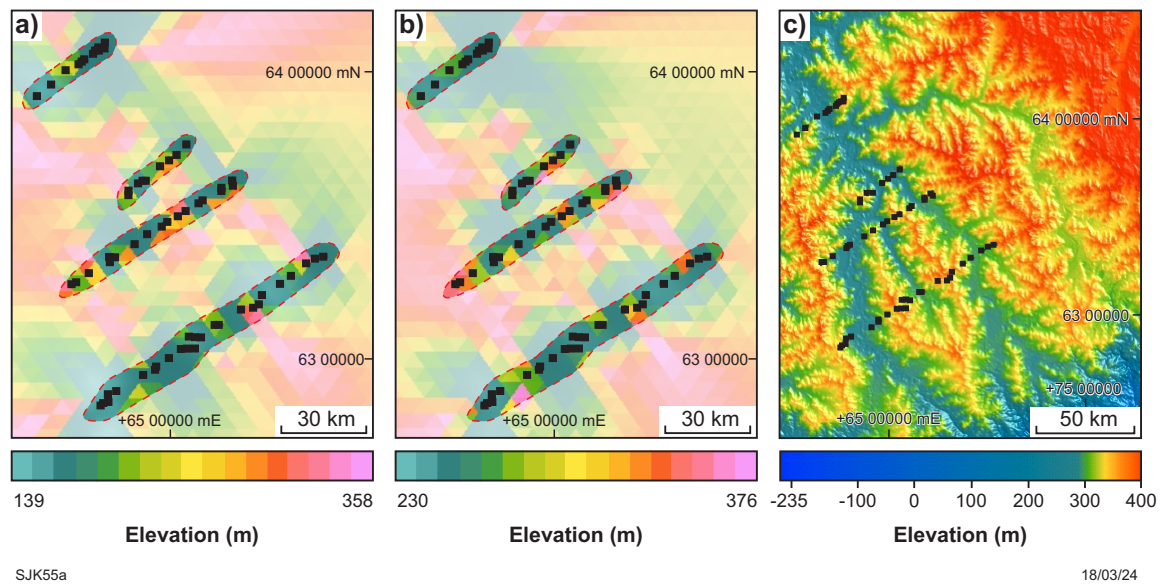


Figure 14. Two velocity models over the study area: a) 520 m/s velocity model; b) 150 m/s velocity model; c) SRTM 1 image of the current landscape. Models in a) and b) have been masked out in the inferred depth-to-basement grid, highlighting the footprints of the HVSR measurements

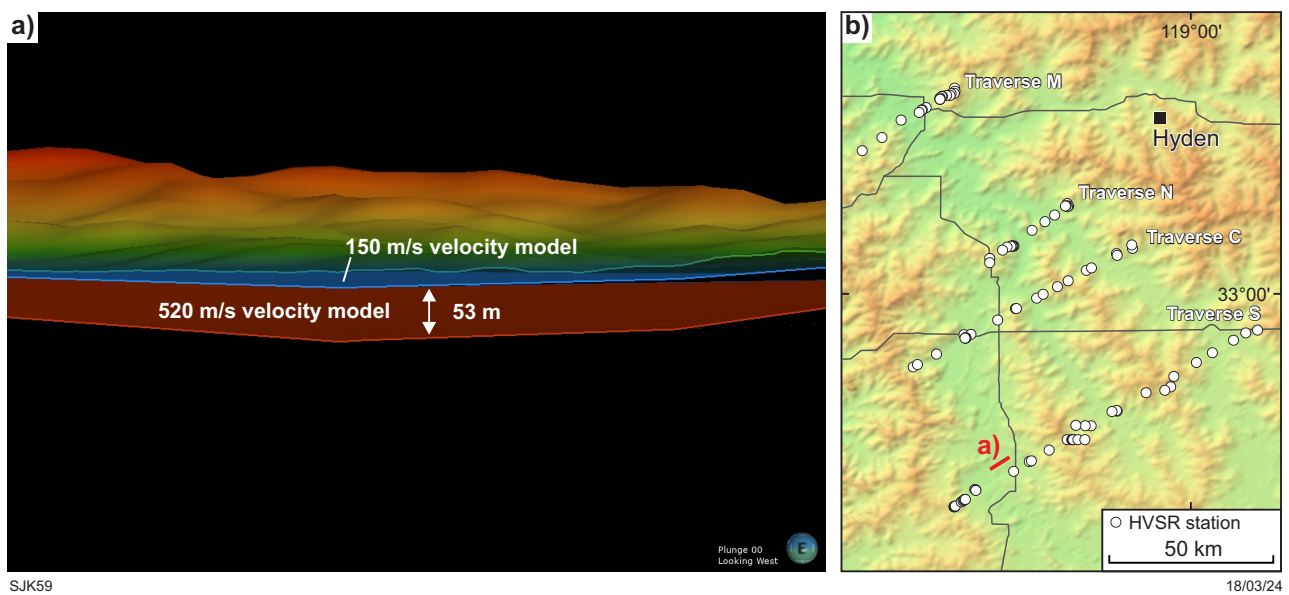


Figure 15. Example showing depth difference between the two velocity models: a) the depth varies from 10 to 53 m across the study area; b) locality map

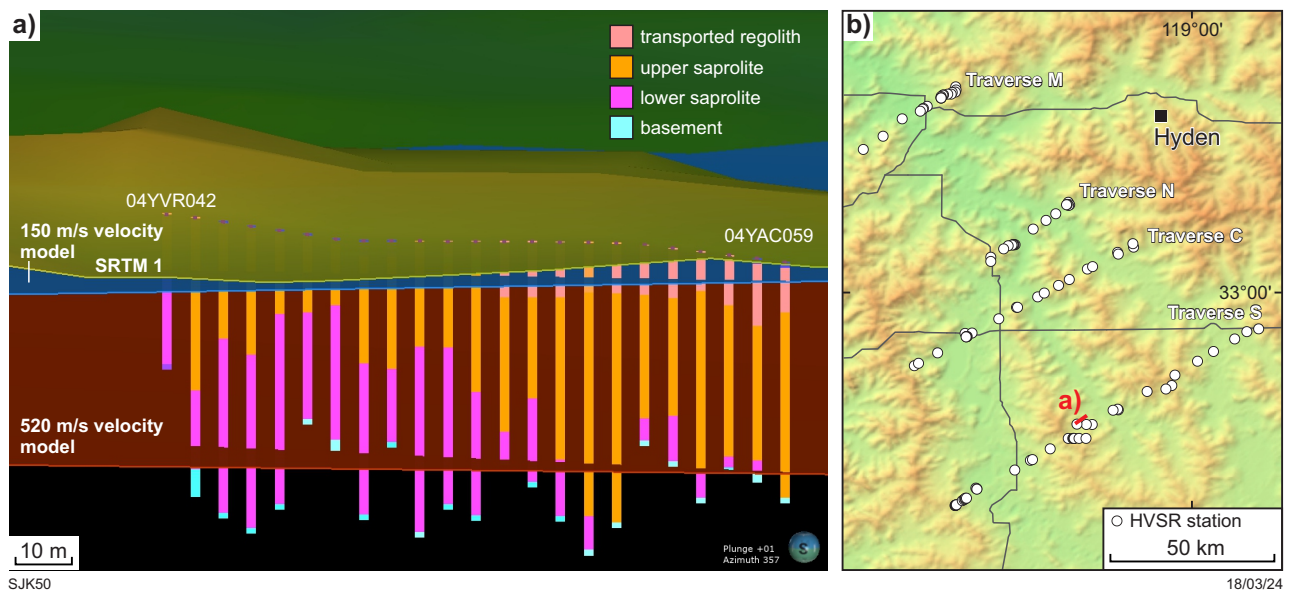


Figure 16. Profile view of the two velocity models compared to lithological intersections by numerous drillholes in the vicinity of Traverse S: a) showing that the 520 m/s model matches much better with the drilling; b) locality map

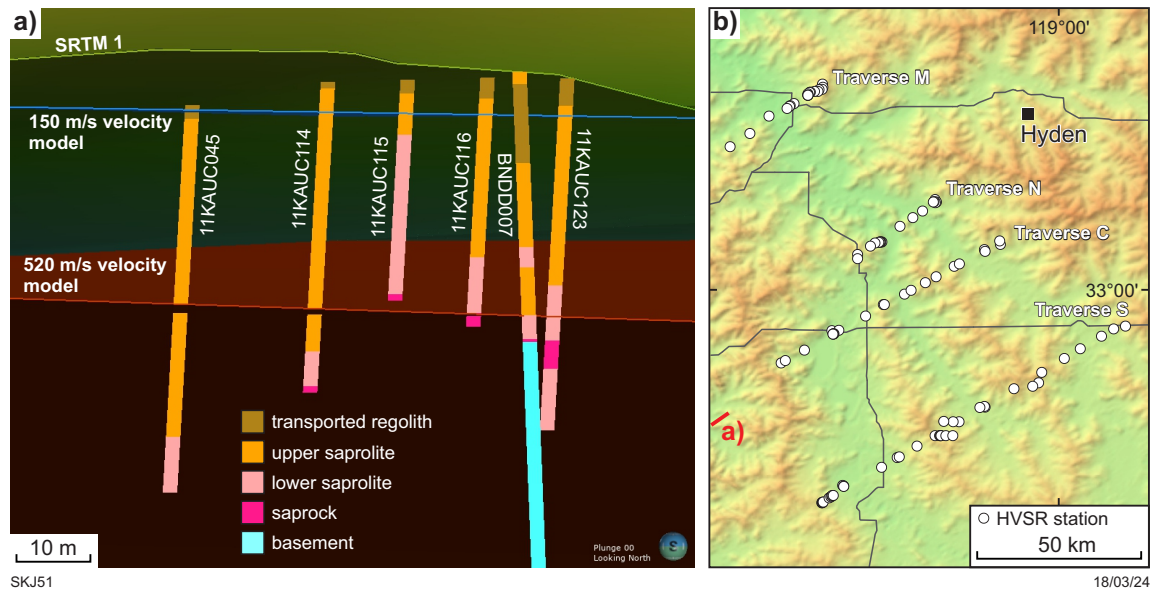


Figure 17. Profile view of the two models against the drilling south from Traverse C: a) the 520 m/s velocity model matches the drilling within 3–15 m accuracy. The discrepancy of the 150 m/s velocity model is greater than 30 m at all six drilling locations; b) locality map

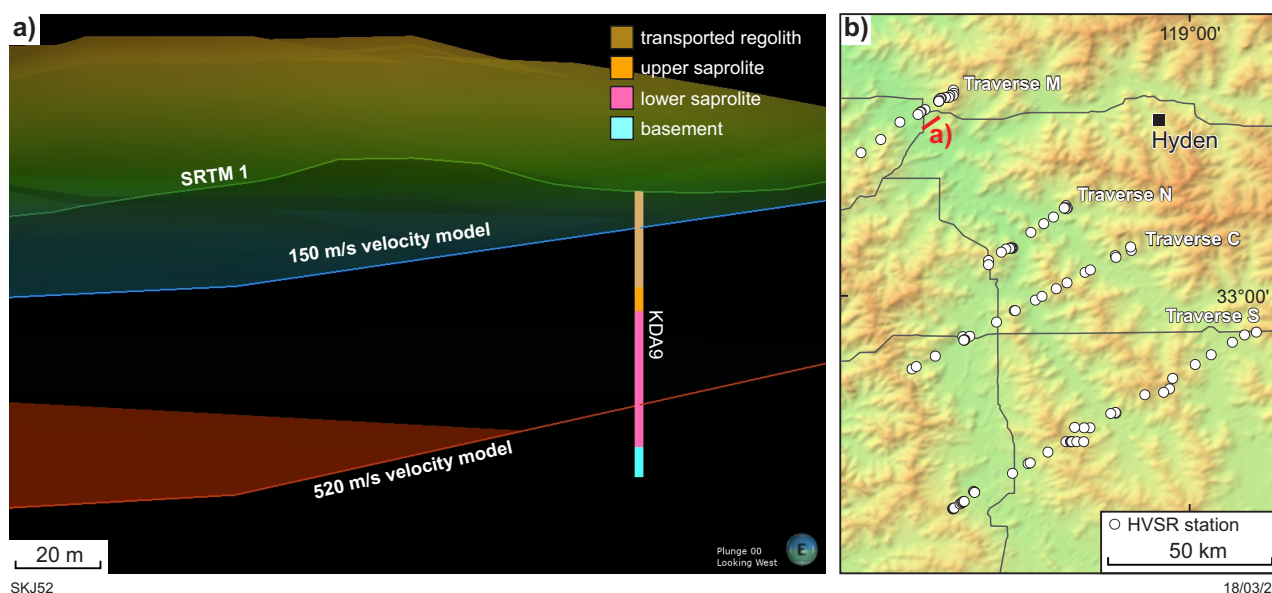


Figure 18. Profile view of the two velocity models 10 km southeast from the northeastern part of Traverse M demonstrating: a) the 520 m/s velocity model (red surface) provides a better match with the drilling results (drillhole KDA9) in the area compared to the 150 m/s model (blue surface). The SRTM 1 surface is also displayed; b) locality map

The results indicate that the 520 m/s velocity model is in better agreement with the drilling data for most of the study area except for Traverse M. Drilling data available near Traverse M showed that 150 m/s velocity model is in much better agreement with the drilling than the 520 m/s model. Here, a third velocity model, which is a combination of the previous two models, is introduced. This new model, named here the hybrid model, used 520 m/s velocity for all recordings throughout the study area, except along Traverse M, where the 150 m/s model was applied (Fig. 20). This hybrid model provides the best correlation between passive seismic data and the available drillhole data over the entire study area.

For example, the profile image of velocity models along Traverse M, near station M17DH HVSr shows that the hybrid model is within 0.7 to 5 m accuracy of basement depths (Fig. 21a). At the same location, the 150 m/s velocity model is within 2–12 m accuracy of basement depths as indicated by drilling. At drillhole BNDD07, the hybrid model is within 2 m accuracy of the basement depth, while the 520 m/s velocity model is within 2.5 m (Fig. 21b). In the southern part of the study area, the hybrid model and 520 m/s models exhibit spatial congruence (Fig. 21c1,c2).

Discussion

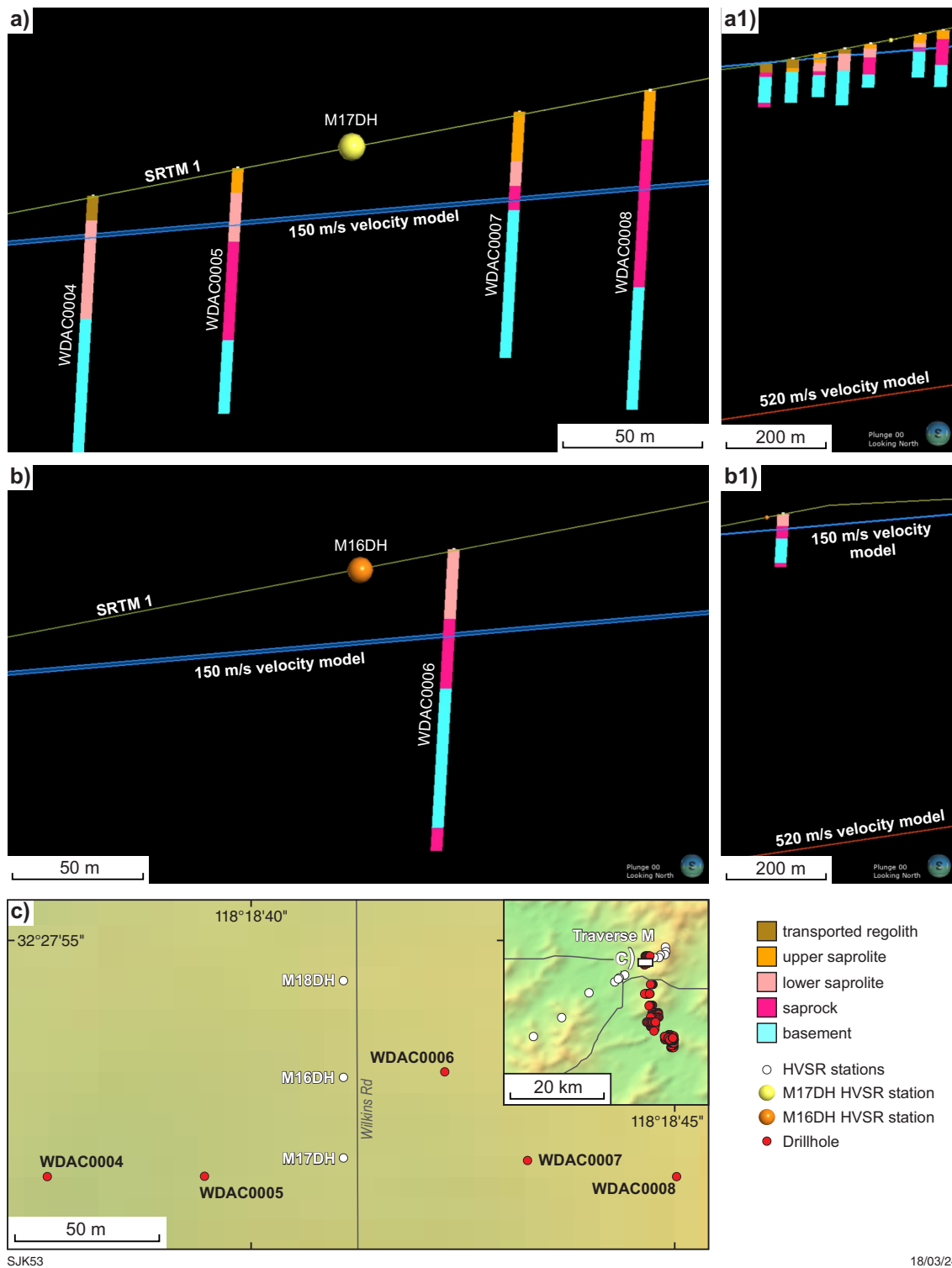
The HVSr passive seismic technology is a cost-effective and time-efficient method for mapping the depth to the crystalline basement, as well as for mapping the geometry and depth of paleochannels. However, like any other geoscientific method it has limitations and challenges. HVSr resolution decreases with depth. Due to the high uncorrelated noise at low frequencies, it is not recommended to use HVSr passive seismic methods to measure depths greater than 1000 m. As demonstrated in this study, wet swampy areas should be avoided. This is because S-waves do not propagate elastically under such ground conditions.

HVSr acquisition, if possible, should further be avoided in heavy rain and under very windy conditions. Strong gusty winds, heavy traffic and construction sites produce excessive signal or vibration that masks the HVSr results, especially at shallower depths. This proved to be particularly difficult when HVSr data were acquired near busy roads and in the areas of hard consolidated ground, such as residual lateritic profiles (e.g. cemented pisolithic ground conditions). Under such conditions, it is very difficult to penetrate consolidated ground with the Tromino device's spikes, in which case the devices need to be placed on the surface using short spikes. Unfortunately, due to insufficient coupling with the spikes, and significant space between the Tromino instrument and the ground, the seismometer records greater amounts of unwanted and uncorrelated noise that can potentially mask observations of stratigraphic signals.

Due to its dependency on the density and velocity of the rock layers, the HVSr method works best when there is a distinct change between different rock sequences. If the change from saprolite to saprock or basement is gradational, the corresponding HVSr peaks will be very subtle or nonexistent.

Furthermore, the HVSr method applies drillhole calibration for local survey conditions. If no drilling data are available, the velocities can be modelled, especially for the shallower geological sequences, by applying MASW (multi-channel analysis of surface waves) or other velocity analyses.

While acknowledging the limitations and challenges listed above, the main challenge in this study was the sparsity of the passive seismic data and the lack of velocity control over the acquired data. Due to restricted access to private farmland, many measurements had to be placed near busy roads or in wet, swampy ground. This resulted in faulty recordings or recording of many noisy data that were challenging to process. Another possible issue that arose, especially in the northern part of the survey, was near-surface granitic rock that masked the actual basement depth.



SJK53

18/03/24

Figure 19. Profile view of two velocity models near the HVSR recording stations M16DH and M17DH: a) profile view at HVSR station M17DH. Only the 150 m/s velocity model is visible; a1) the 520 m/s velocity model is too deep and shown here; b) profile view near HVSR station M16DH. Only the 150 m/s velocity model is visible; b1) the 520 m/s velocity model is too deep and shown here; c) locality map for a) and b)

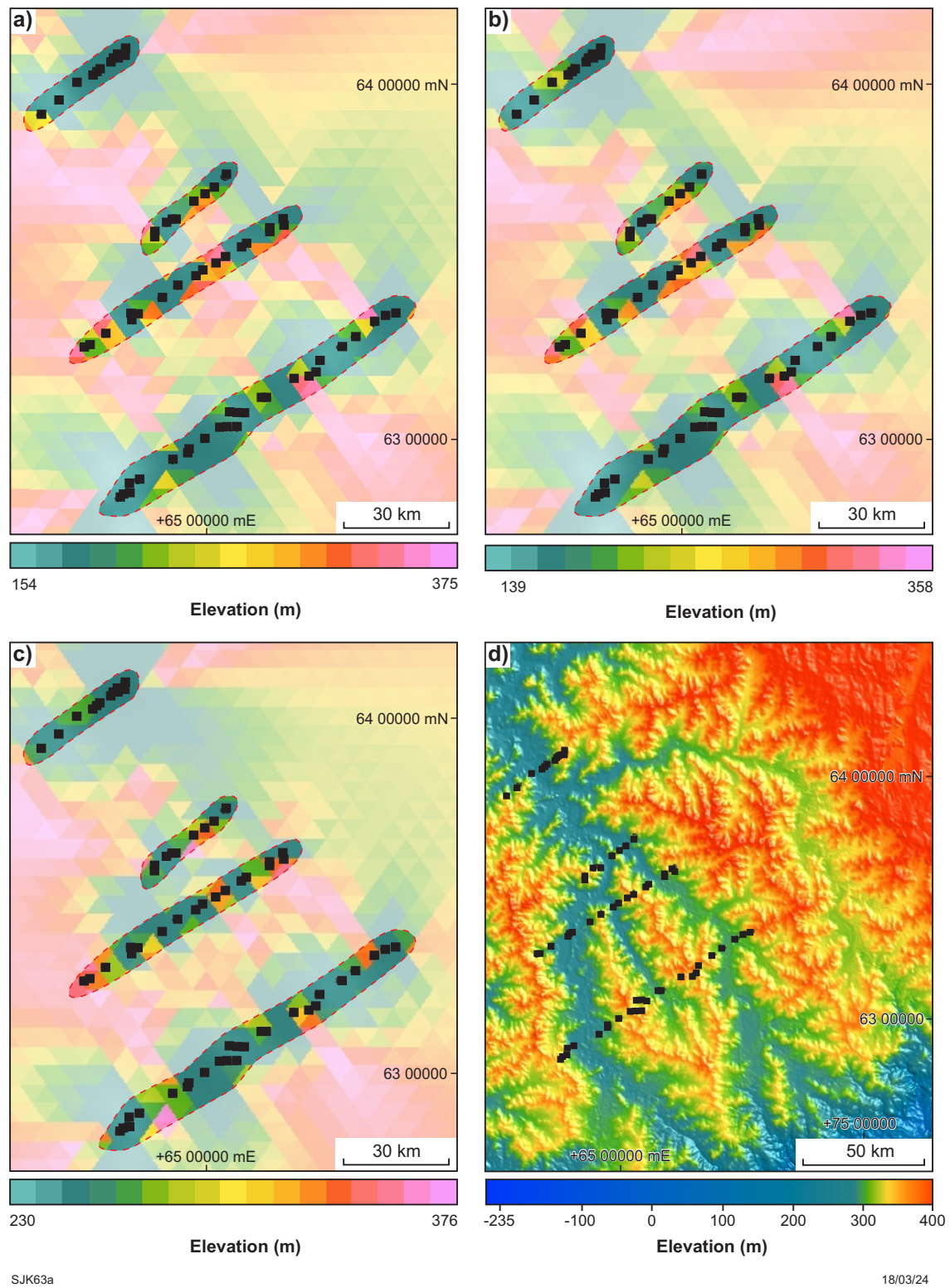


Figure 20. Plan view of three velocity models: a) hybrid model; b) 520 m/s velocity model; c) 150 m/s velocity model; d) SRTM 1 image of the study area. All three models follow the general geometry of the study area as seen in the SRTM 1 image. The locations of HVSR stations are displayed as black squares. The visualisation of all 3 models has been masked out in the inferred depth-to-basement grid, highlighting the footprints of the HVSR measurements. The masked area is less reliable, as HVSR provides inference of 1D structure

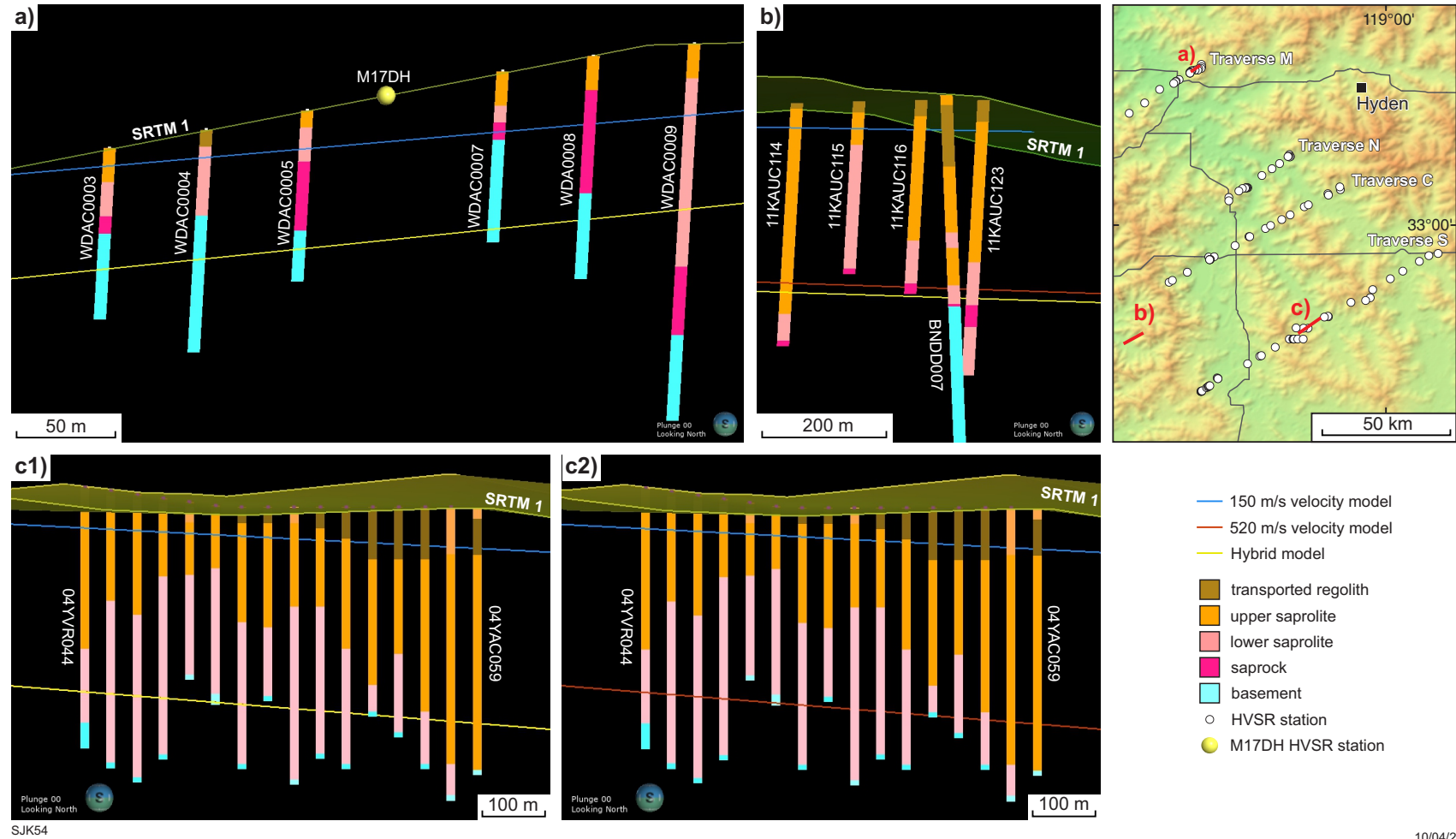


Figure 21. Profile view of three velocity models at three locations for comparison: a) along Traverse M near HVSr station M17DH, the hybrid model provides a better match with basement depths than the 150 m/s velocity model. Note that the 520 m/s velocity model is too deep for this scale and is not shown in this example; b) profile view of three velocity models to the southwest from Traverse C; c) three velocity models along Traverse S. In this case, both the hybrid and 520 m/s models are the same; c1) hybrid; c2) 520 m/s velocity model. Locality map is shown

10/04/24

Despite these factors, the HVSR method proved to be a useful approach for defining the geometry of the paleochannels and mapping the depth to the crystalline basement in the study area.

Our main recommendation for future work is to apply the HVSR method to smaller study areas using a denser array of passive seismic stations and to have access to accurate, independently acquired velocity constraints. When applied on a larger regional scale, as demonstrated in this study, the method would yield the best results when combined with other geophysical methods such as airborne electromagnetic (AEM) surveys. This is especially important for interpreting areas between passive seismic traverses, such as the 40 km spacing between AEM lines in southwestern Western Australia. Jakica et al. (2021) demonstrated in their study of the Yangibana paleochannel in the Gascoyne region of Western Australia that a paleochannel's geometry can be accurately mapped when HVSR, AEM, gravity and ground electromagnetic data are used together, which results in a much more detailed model.

Conclusions

This study demonstrates the efficient use of the HVSR passive seismic method in regional settings where modelling the depth to basement is necessary. Despite limited ground access and resulting sparse data acquisition, a geologically meaningful depth-to-basement model was produced. In general, areas of surface drainage show an increase in depth to basement (i.e. cover thickness), likely due to the geometry of paleovalleys at different orders of branching.

Three velocity models were produced, with the hybrid model being identified as the optimal model. The hybrid model displayed satisfactory concurrence with drillhole data within the range of 0.4 to 10 m across HVSR traverses. Notably, due to the implicit modelling and the sparse spacing between the four HVSR traverses, the disparity between the model and drilling outcomes escalates with increasing distance from these traverses.

To improve the geological model, additional passive seismic data should be collected from strategic areas of the study area, such as infill stations along a single traverse line, new traverses parallel and between existing ones, and a few traverses oriented perpendicular to existing southwest–northeast lines. Additionally, integrating geophysical data such as AEM can improve the depth-to-basement model. With drilling limitations in the area, an MASW (multi-channel analysis of surface waves) survey is recommended to obtain seismic velocity readings at shallower depths.

Overall, the study provides valuable insights into using the HVSR method for cost-effective surveying and time-efficient interpretation of depth-to-basement variations in regions with limited access to measurement sites. The recommendations outlined in this study can aid in improving the geological models in the study area and can be extended to other regions with similar characteristics.

Acknowledgements

We are especially thankful to the Minerals Research Institute of Western Australia (MRIWA), Anglo American Ltd and Ramelius Resources Ltd for their support of this work through the MRIWA 10433 Project. The Commonwealth Scientific and Industrial Research Organisation (CSIRO) is thanked for its support and providing the 19 Tromino instruments used in this study. Andrew King (CSIRO) is thanked for the preparation of the CSIRO Tromino instruments prior to the field experiment. John O'Donnell and Matt Clarke are thanked for their insightful reviews.

References

- Anand, RR and Butt, CRM 2010, A guide for mineral exploration through the regolith in the Yilgarn Craton, Western Australia: Australian Journal of Earth Sciences, v. 57, p. 1015–1114.
- Asten, MW 2004, Passive seismic methods using the microtremor wave field, in ASEG Extended Abstracts: ASEG 17th Geophysical Conference, Sydney, ASEG Extended Abstracts 2004, p. 1–4.
- Chandler, VW and Lively, RS 2014, Evaluation of horizontal-to-vertical spectral ratio (HVSR) passive seismic method for estimating the thickness of Quaternary deposits in Minnesota and adjacent parts of Wisconsin: Minnesota Geological Survey, Open File Report 14-01, 52p.
- Cherry, J, 2020, C81/2018, E70/5018, E70/5019, E70/2020 and E70/5021 Final Surrender Report for the period ending 21/03/2020: Cygnus Gold Limited Report: Geological Survey of Western Australia, Statutory mineral exploration report A123856, <www.dmir.wa.gov.au/wamex>, 19p.
- Collins, C, Kayen, R, Carkin, B, Allen, T, Cummins, P and McPherson, A 2006, Shear wave velocity measurement at Australian ground motion seismometer sites by the spectral analysis of surface waves (SASW) method: Earthquake Engineering in Australia, p. 173–178.
- Commander, DP 1989, Western Australia groundwater salinity map: Geological Survey of Western Australia, 1:10 000 000.
- Cornelius, M, Robertson, IDM, Cornelius, AJ and Morris, PA 2007, Laterite geochemical database for the Western Yilgarn Craton, Western Australia: Geological Survey of Western Australia, Record 2007/9, 44p, doi: 10.4225/08/586009a364f32.
- de Broekert, P and Sandiford, M 2005, Buried inset-valleys in the eastern Yilgarn Craton, Western Australia: Geomorphology, aged, and allogenic control: The Journal of Geology, v.113, p.471–493.
- de Souza Kovacs, N 2022, Laterite element concentration relationship to major crustal structures in the Southwest Yilgarn Craton: Curtin University, Bentley, Western Australia, Master of Science thesis (unpublished), 74p.
- de Souza Kovacs, N and Jakica, S 2021, 1:100 000 Regolith geology regimes of Western Australia (1:100 000): Geological Survey of Western Australia, 1:100 000 Geological Series.
- Delgado, J, López Casado, C, Estévez, A, Giner, J, Cuenca, A and Molina, S 2000, Mapping soft soils in the Segura river valley (SE Spain): A case study of microtremors as an exploration tool: Journal of Applied Geophysics, v. 45, p. 19–32.
- Feldpausch, SA 2017, Gravity and Passive Seismic Methods Used Jointly for Understanding the Subsurface in a Glaciated Terrain: Dowling and Maple Grove Quadrangles, Barry Country, Michigan, no. 923: Western Michigan University, Michigan, USA, Master of Science thesis (unpublished), 90p.

- Gallant, J and Austin, J 2011, Multi-resolution Valley Bottom Flatness (MrVBF) derived from 1 second DEM-S: CSIRO.
- Gasson M 2018, E70/4787 Stanley Project Co-funded Government-Industry Drilling Program: Final report for the drilling program ending 26/5/18: Cygnus Gold Limited: Geological Survey of Western Australia, Statutory mineral exploration report A117455, <www.dmirs.wa.gov.au/wamex>, 21p.
- Gee, RD, Baxter, JL, Wilde, SA and Williams, IT 1981, Crustal development in the Archean Yilgarn Block, Western Australia, in *Archean Geology: Second International Symposium, Perth 1980* edited by JE Glover and DI Groves: Geological Survey of Australia, Special Publication 7, p. 43–56.
- Gee, RD, Myers, JS and Trendall, AF 1986, Relation between archaean high-grade gneiss and granite-greenstone terrain in western Australia: *Precambrian Research*, v.33, no.1, p. 87–102, doi:10.1016/0301-9268(86)90016-1, <www.sciencedirect.com/science/article/pii/0301926886900161>.
- González-Álvarez, I, Salama, W and Anand, RR 2016, Sea-level changes and buried islands in a complex coastal palaeolandscape in the South of Western Australia: implications for greenfields mineral exploration: *Ore Geology Reviews*, v. 73, p. 475–499, doi:10.1016/j.oregeorev.2015.10.002.
- Hirschmann, C 2008, Newdegate Project Yandina E70/2397 from 10 October 2003 to 9 October 2007, South West Mineral Field: Map Sheets: Newdegate SI50-8 1:250 000, Burangup 263 1:1000 000, Albany SI50 1:1000 000, Partial Surrender Report, CAN no 000 6600 864: Dominion Mining Limited, Perth: Geological Survey of Western Australia, Statutory mineral exploration report A78275, <www.dmirs.wa.gov.au/wamex>, 12p.
- Hou, B, Frakes, LA, Sandiford, M, Worrall, L, Keeling, J and Alley, NF 2008, Cenozoic Eucla Basin and associated palaeovalleys, southern Australia-- climatic and tectonic influences on landscape evolution, sedimentation and heavy mineral accumulation: *Sedimentary Geology*, v. 203, p. 112–130.
- Ibs-von Seht, M and Wohlenberg, J 1999, Microtremor measurements used to map thickness of soft sediments: *Bulletin of the Seismological Society of America*, v. 89, no. 1, p. 250–259.
- Jakica, S, Brisbourn, L and de Souza Kovacs, N 2021, Applying geophysics for 3D paleochannel imaging in the Gascoyne Province, Western Australia: Geological Survey of Western Australia, Record 2021/7, 27p.
- Kumar, M, Hart, J and Prakash, N 2018, Application of passive seismic in determining overburden thickness: North West Zambia, in *AEGC Extended Abstract 2018: Australian Exploration Geoscience Conference, Sydney*, 18–21 February 2018.
- Lane, JW, White, EA, Steele, GV and Cannia, JC 2008, Estimation of Bedrock Depth Using the Horizontal-to-Vertical (H/V) Ambient-Noise Seismic Method, in *Symposium on the Application of Geophysics to Engineering and Environmental Problems, Proceedings: Symposium on the Application of Geophysics to Engineering and Environmental Problems 2008*, Philadelphia, Pennsylvania, Denver, Colorado, 6–10 April 2008: Society of Exploration Geophysicists, doi.10.4133/1.2963289.
- Magee, J 2009, Palaeovalley groundwater resources in arid and semi-arid Australia-- a literature review: *Geoscience Australia, Record 2009/3*, 224p.
- Meyers, J 2017, Passive seismic surveying background, methods and HVSR case studies: Australian Institute of Geoscientists; AIG Workshop, 2 May 2017, Brisbane, Queensland, www.aig.org.au/wp-content/uploads/2017/06/01_Passiveintro_Meyers.pdf.
- Micromed 2009, The Short Tromino How To: What should I do now? MOHO Science and Technology, Treviso, Italy, 26p.
- MoHo 2017, Tromino Portable ultra-light acquisition system for seismic noise and vibrations: User's Manual: MoHo Science and Technology, Venice, Italy, 148p., <www.moho.world>.
- Myers, JS 1993, Precambrian history of the Western Australian Craton and adjacent orogens: *Annual Review of Earth and Planetary Sciences*, v. 21, p. 453–485.
- Nakamura, Y 1989, A method for dynamic characteristics estimation of subsurface using microtremor on the ground: *Quarterly Report of the Railway Technical Research Institute*, v. 30, no. 1, p. 25–33.
- Owers, MC, Meyers, JB, Siggs, B and Shackleton, M 2016, Passive seismic surveying for depth to base of paleochannel mapping at Lake Wells, Western Australia: 25th International Geophysical Conference and Exhibition, Adelaide, South Australia, 21–24 August: Australian Society of Exploration Geophysicists, ASEG Extended Abstracts 2016, 9p.
- Pernreiter, S, González-Álvarez, I, Klump, J, Smith, G and Ibrahim, T 2018, Landscape evolution in the south Yilgarn Craton and Albany–Fraser Orogen, Western Australia. CSIRO Internship Thesis, Mineral Resources, Discovery Internship Program, Australia, EP183453, 67p.
- Quentin de Gromard, R, Ivanic, TJ and Zibra, I 2021, Pre-Mesozoic interpreted bedrock geology of the southwest Yilgarn, 2021, in *Accelerated Geoscience Program extended abstracts compiled by Geological Survey of Western Australia: Geological Survey of Western Australia, Record 2021/4*, p. 122–144.
- Reddy, D 2011, Annual Report Rock Dam Hill Project E70/2828 Kent Shire, Western Australia: Reporting period 28 May 2012 to 27 May 2011: Magnetic Resources: Geological Survey of Western Australia, Statutory mineral exploration report A90574, <www.dmirs.wa.gov.au/wamex>.
- Scheib, AJ 2014, The application of passive seismic to estimate cover thickness in greenfields areas of Western Australia – method, data interpretation and recommendations: Geological Survey of Western Australia, Record 2014/9, 67p.
- Scheib, AJ, Morris, P, Murdie, R and Delle Piane, C 2016, A passive seismic approach to estimating the thickness of sedimentary cover on the Nullarbor Plain, Western Australia: *Australian Journal of Earth Sciences*, v. 63, no. 5, p. 583–598, doi:10.1080/08120099.2016.1233455.
- SESAME European Research Project 2004, Guidelines for the implementation of the H/V spectral ratio technique on ambient vibrations-- measurements, processing and interpretation: European research project WP12-- Deliverable D23.12: European Commission-- Research General Directorate, 62p.
- Sowerby, RD and Mills, MB 1998, Final Exploration Report for work carried out by North Limited on E70/1555 (Kondinin Joint Venture) for the period 27 March 1997 to 18 September 1998: Report No. WA99/13S: North Limited: Geological Survey of Western Australia, Statutory mineral exploration report A56202, <www.dmirs.wa.gov.au/wamex>, 23p.
- Spaggiari, CV, Kirkland, CL and Smithies, RH 2017, Regional geology and metallogeny of the Albany–Fraser Orogen, in *Australian Ore Deposits* edited by GN Phillips: Australasian Institute of Mining and Metallurgy, Monograph 32, p. 385–388.
- Tolson, A 2011, Kuerin Project Group Annual Report (C127/2006) E70/2835, E70/2836, E70/2837, E70/2839, and E70/2840: from 1st April 2010 to 31 March 2011: Kingsgate Consolidated Limited: Geological Survey of Western Australia, Statutory mineral exploration report A90254, <www.dmirs.wa.gov.au/wamex>, 18p.
- Tyrer, MA 1980, Katanning Project, Annual Report for the period ending 1st May 1980, MCs70/18808-18815, 18818-18826, 18837-18878, 18884-18911, 18959-18973, 19046, 19085-19088: GML70/146-157, 218225: Otter Exploration NL: Geological Survey of Western Australia, Statutory mineral exploration report A9265, <www.dmirs.wa.gov.au/wamex>, 205p.
- USGS 2014, Shuttle Radar Topography Mission (SRTM) 1 Arc-Second Global (Global scale): United States Geological Survey, www.usgs.gov.
- Wilde, SA, Middleton, MF and Evans, BJ 1996, Terrane accretion in the southwestern Yilgarn Craton: Evidence from a deep seismic crustal profile: *Precambrian Research*, v. 78, no. 1–3, p. 179–196.

IMAGING THE GEOMETRY OF PALEOVALLEYS IN THE SOUTHWEST
REGION OF WESTERN AUSTRALIA: LINKING BASEMENT AND COVER

S Jakica, P Duuring, I González-Álvarez and JK Porter

The southwestern region of Western Australia features a regolith-dominated terrain, posing challenges in understanding its cover architecture. Non-invasive geophysical techniques, particularly the HVSR passive seismic method, offer an efficient means to map regolith sequences and estimate cover thickness economically. This study evaluates the effectiveness of deploying Tromino seismometers over four days to gather HVSR data and interpret depth-to-basement variations, notably in paleovalley settings. The report elucidates the HVSR method's principles and its application in paleovalley settings, detailing methodology from planning traverses to data collection with Tromino seismometers. The findings aim to promote wider adoption of HVSR techniques across Western Australia. The study presented in this metadata report is the result of a collaborative research project, Detection of Distal Footprints of Minerals Systems in the southwest of Western Australia: Linking basement and Cover (SOWETO), with the Geological Survey of Western Australia (GSWA), Commonwealth Scientific and Industrial Research Organisation (CSIRO), Minerals Research Institute of Western Australia (MRIWA), Anglo American Ltd and Ramelius Resources Ltd.



Further details of geoscience products are available from:

First Floor Counter
Department of Energy, Mines, Industry Regulation and Safety
100 Plain Street
EAST PERTH WESTERN AUSTRALIA 6004
Phone: +61 8 9222 3459 Email: publications@dmirs.wa.gov.au
www.demirs.wa.gov.au/GSWApublications